Correlating Aeroacoustic Measurements and Predictions

Eric Manoha
Computational Aeroacoustics Research Unit
Aerodynamics, Aeroelasticity and Acoustics Department
ONERA, Châtillon
FRANCE

eric.manoha@onera.fr

ABSTRACT

Aircraft noise prediction and reduction require a good balance between numerical simulation and experiment. Both approaches are definitely complementary: experiments are necessary to validate computations, and computations are useful to design and interpret experiments. However, correlating experimental and numerical aeroacoustic results is generally challenging because flow and acoustic propagation conditions never perfectly match in experimental and computational set-ups of a given configuration. In this lecture, we present several examples showing how the influence of these differences can be mitigated or corrected. These examples were collected from several projects devoted to the characterization of the reduction of aircraft main noise sources, in various aerodynamic and acoustic facilities.

1. CONTEXT

External noise generated by large transport aircraft typically includes engine noise (propeller, fan, jet, turbine, compressor, combustion) and airframe noise (high lift systems, landing gear, cavity) (Figure 1, left). Moreover all noise sources are subjected to installation effects, which means that they interact with the airframe structure with possible acoustic reinforcement or shielding (Figure 1, right).

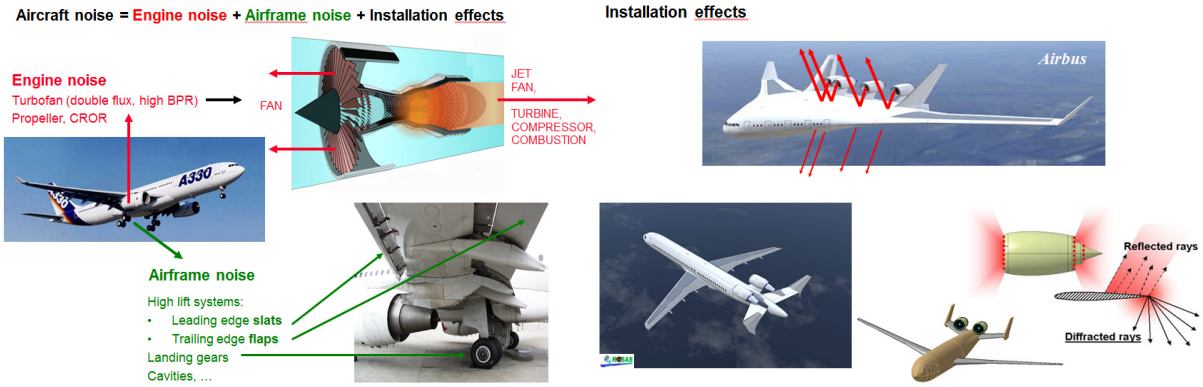

Figure 1 - Left : main noise sources for large transport aircraft
Right: acoustic engine installation effects

Aircraft noise reduction increasingly relies on predictions achieved via numerical simulation. In this context, validation tools are critical for the assessment of numerical methods. However, the validation of numerical methods through theoretical or analytical models is very limited. For realistic geometries and physical mechanisms, experiment remains mandatory. Nevertheless, access to dedicated experimental database is recent. For example, in the context of EU funded research on aircraft engine (fan and jet) noise

reduction in the last 15 years, there has been a good balance between (i) projects on experimental and semi-empirical techniques (SILENCER, VITAL, OPENAIR) and (ii) projects on numerical simulation methods including experimental validation (JEAN, COJEN TurboNoiseCFD, TURNEX and FLOCON). In the thematic of airframe noise prediction and reduction, most funded projects have been devoted to semi-empirical techniques (RAIN, SILENCER, TIMPAN and OPENAIR), whereas the VALIANT project has been the first (and only one) project devoted to the evaluation and amelioration of up-to-date CFD/CAA methods for the prediction of airframe noise generation and radiation, including experimental validation. This situation can be explained by the fact that, since the early 50s, engine noise (with a priority to jet noise) has been the main driver of the acoustic research community, as long as it was considered as the dominant noise source on common transport aircraft. With the continuous progress on engine noise reduction, and the increase in aircraft average size, airframe noise has now become a dominant source, especially during the approach and landing phases, which explains that part of the global effort has been re-oriented to airframe noise prediction and reduction.
It should be underlined that this lack of data is not specific of the aeroacoustic research community in Europe since, in quasi-synchronicity with the VALIANT project, NASA has launched the BANC (Benchmark for Airframe Noise Computations), which objective is to provide the worldwide aeroacoustic community with experimental data for the validation of airframe noise computations.
More recently, in the project IMAGE (now in progress), a new objective is to provide reliable experimental databases for the validation of numerical simulations of innovative noise reduction devices for airframe (turbulence grids, plasma actuators) and engine (liners) noise.

2. HYBRID EXPERIMENTS TO VALIDATE HYBRID SIMULATIONS

Aircraft noise predictions methods are generally hybrid, in the sense that they combine several methods, each one being dedicated to solving a specific physics in a limited domain.
In the near-field, turbulent flow interacts with solid (steady or rotating) surfaces, generating aeroacoustic sources, which are generally simulated using unsteady CFD, solving the Navier-Stokes equation with adequate resolution in the space and time domains.
There is generally a “midfield” region characterized by low turbulence levels (thus, without aeroacoustic sources) but significant mean flow spatial gradients and, possibly, the presence of solid surfaces. In such region, the simulation of acoustic propagation must account for refraction effects through the non-uniform mean flow and the acoustic reflections and scattering on solid surfaces, which can only be done using CAA (Computational AeroAcoustics) methods, for example based on Linearized Euler Equations (LEE).
This “midfield” region is bounded by an external surface, beyond which the mean flow can be considered as uniform. In this “far-field” region, the acoustic radiation up to the observer can rely on integral methods based on an analytic Green function (Figure 2, left side).

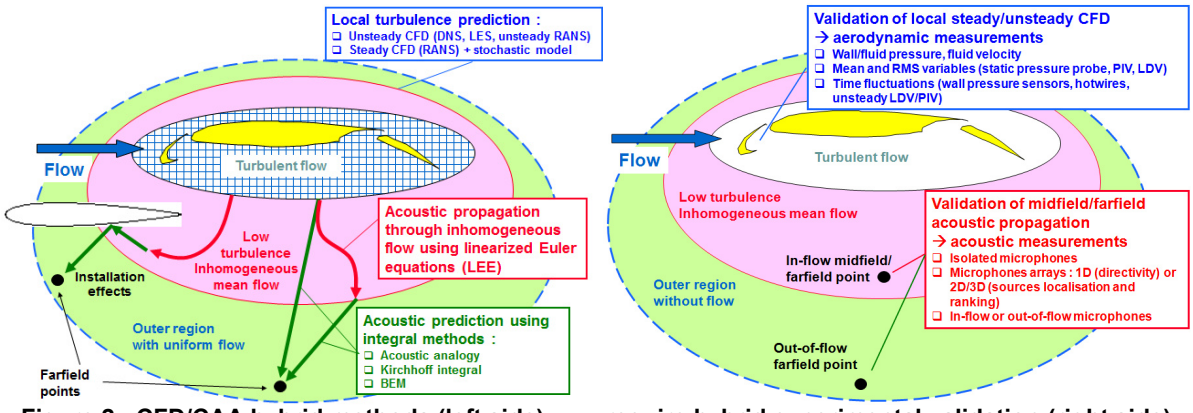

Figure 2 - CFD/CAA hybrid methods (left side) …… require hybrid experimental validation (right side)

The same hybrid character exists for experimental validation as for numerical prediction, in the sense that each successive step of the numerical simulation requires specific measurements for validation (Figure 2,

right side).
The validation of local steady/unsteady CFD requires aerodynamic measurements of wall/fluid pressure and fluid velocity, including:

- Mean and RMS variables, measured by static pressure probe, PIV, LDV
- Time fluctuations, measured by wall pressure sensors, hotwires, unsteady LDV/PIV.

On the other hand, the validation of midfield/farfield acoustic propagation requires acoustic measurements based on specific instrumentation:

- Isolated microphones
- Microphone arrays : 1D (directivity) or 2D/3D (sources localisation and ranking)
- In-flow or out-of-flow microphones

The next section covers the various possible alternatives for the design of an experiment dedicated to the validation of airframe noise numerical predictions, including the model and the facility choice.

3. EXPERIMENTAL ALTERNATIVES

3.1 Model choice

3.1.1 Full aircraft versus isolated component

Depending on what objectives are aimed at, aeroacoustic tests for aircraft noise characterization can be conducted either on full aircraft geometries or on isolated components responsible for aircraft noise generation (jet, fan, propeller, landing gear, cavity, high lift airfoil section).
Tests on full aircraft geometries (either at full scale or at model scale) are generally not the most convenient for CFD/CAA validations, because all aircraft noise sources are combined and mixed-up and, thus, difficult to tell apart. However, full scale aircraft tests are still useful for noise sources identification and ranking, including the acoustic installation effects of the aircraft structure/airframe on the radiation of the sources. Moreover, unsteady CFD of full aircraft flow is still out-of-reach, even at small scale.
Consequently, most aircraft noise numerical predictions are generally limited to isolated components, either for academic configurations (simple jet, isolated propeller, tandem cylinders, rod-airfoil), or for realistic components (landing gears, high lift wings and airfoils, cavities). The main drawback of this approach is that it generally excludes acoustic installation effects.

3.1.2 Full scale versus model scale

The choice of the scale affects both the numerical simulations and the corresponding validation experiment. Numerical simulations are often limited to small scale because the computational cost dramatically increases with the Reynolds number. In that sense, for given computational capacities, the "isolated component" approach allows larger scales and, thus, more realistic Reynolds numbers.

3.2 Facility choice

3.2.1 Open space versus windtunnel

Aeroacoustic tests in open space are generally limited to flyover measurements with full aircraft, most often at full scale, but also possible at model scale using remotely controlled flying models. The main advantage is that the aerodynamic and acoustic conditions are inherently very realistic. However, this is obtained at the price of a significant dependency to the outdoor weather conditions and, thus, a rather poor repeatability. On the other hand, measurements in windtunnel allow a good control of the test conditions for repeatability, but are always biased by side-effects like acoustic and aerodynamic installation effects.
Experimentalists in aeroacoustics generally classify windtunnels in three categories.

3.2.2 Closed test section windtunnels

The facilities with closed test sections are generally designed for aerodynamic measurements, with aerodynamic conditions which are close (but not identical) to free field conditions. Since most CFD activities also generally assume aerodynamic free field conditions, these facilities are the best to validate CFD (steady/unsteady) computations. On the other hand, acoustic measurements are often problematic in

such windtunnels because of (generally) high background noise and acoustic confinement due to hard walls, floor and ceiling.

3.2.3 Open-jet windtunnels

The other category concerns windtunnels with open test section, in which a nozzle generates an open jet in a large room. If the room walls are equipped with absorbent liners for anechoicity, and if the background noise is low enough, this kind of facility offers acoustic conditions closer to free field conditions. In that sense, acoustic measurements in open jet windtunnels are the best to validate acoustic predictions. In the other hand, these facilities generally do not offer the best aerodynamic conditions, especially with lifting models which tend to deflect the open jet. Moreover aerodynamic measurements are practically more difficult in these facilities, due to the absence of near walls to support the instrumentation.

3.2.4 Hybrid aeroacoustic windtunnels

A third category has recently emerged, as a tentative compromise between open-jet and closed section facilities. The "hybrid" windtunnel is generally a former closed section aerodynamic windtunnel which has been refurbished into an aeroacoustic facility,

- firstly by significantly reducing the background noise by any possible device (mufflers, liners, silent engine and fan),
- secondly by replacing the vertical lateral hard walls by acoustically transparent stretched Kevlar or wire-mesh cloths and
- finally, adding two anechoic chambers beyond each Kevlar wall, in which acoustic instrumentation is located.

The floor and ceiling are typically covered with absorbent liners to suppress noise reflections. Such hybrid aeroacoustic facility is assumed to provide aerodynamic conditions very close to a hard-walled closed section windtunnel with rather good acoustic conditions (anechoicity and low background noise). A good example of such hybrid facility is the new Virginia Tech Anechoic Wind Tunnel [1].

3.3 Possible experimental strategies

The choice of a model and a scale actually depends on the numerical simulation that is expected to be validated. However, since most unsteady CFD simulations are limited to an isolated aircraft component, one will prefer to test only this component in windtunnel(s) at the largest possible scale with respect to the Reynolds similitude. Now let us summary the possible strategies for the choice of the windtunnel(s) for the achievement of combined aerodynamic and acoustic tests on a given model and set-up.

3.3.1 Aerodynamic/acoustic tests in a single wind tunnel with closed test section

The first option is to perform all tests with the model mounted in a single aerodynamic windtunnel with a closed test section. This option is actually the best for CFD validation (especially since most CFD are achieved in free field conditions). On the other hand, acoustic measurements will be, to a given extent, biased by confinement effects (multiple reflections on hard walls). Moreover, most aerodynamic closed section windtunnels were originally not designed with constraints of silent operation, so acoustic measurements could be disturbed (or even jeopardized) by excessive background noise. Thus acoustic experimental data will be difficult to compare with numerical predictions, unless:

- acoustic measurements are corrected from these confinement effects, for example by using beamforming techniques with "de-noising" and "de-reverberating" process or
- acoustic numerical predictions account for them, for example using BEM or CAA methods including the windtunnel walls (which excludes integral methods).

Beyond the question of validating the prediction methods, it should be underlined that, despite all the apparent drawbacks of this strategy, it remains very attractive to industrial partners. Indeed, since accurate aerodynamic tests of complete aircraft are still mandatory for any new aircraft project, it makes sense to try to collect acoustic data during the same experiment, with only a limited added cost.

3.3.2 Aerodynamic/acoustic tests in an hybrid windtunnel

An alternative to the last option intents to take benefit from the recent concept of hybrid aeroacoustic windtunnel, a closed section windtunnel in which lateral hard walls have been replaced by acoustically

transparent Kevlar fabric, adjacent to anechoic chambers. This is theoretically the best option for both aerodynamic and acoustic measurements but, unfortunately, such facilities are still rare.

3.3.3 Aerodynamic/acoustic tests in a single open test section (anechoic/silent) WT

The second option is to perform all tests with the model mounted in a single acoustic (which means, silent and anechoic) open test section wind tunnel. The main risk of this option is that, due to aerodynamic installation effects the actual flow around the model is generally different from the flow that is computed with CFD based of free-field conditions. The first consequence is that such test can be of limited interest for the validation of CFD method, unless the CFD accounts for the exact 3D aerodynamic conditions of the open-jet facility, which is more and more possible for the mean flow (using RANS method) but generally out-of-reach for unsteady flow. The second consequence is that the numerical prediction of farfield noise based on these free-field CFD results could be very different from the noise actually measured in the windtunnel.

In the other hand, if the flow computation accounts for the actual aerodynamic conditions, then the test set-up will be the most adequate for the validation of acoustic predictions achieved in free field conditions, as long as corrections of refraction through the WT jet shear layer are applied.

3.3.4 Aerodynamic tests in closed test section, acoustic tests in open test section

This option is to (legitimately) try to take benefit of the advantages of each strategy, thus to successively test the same model in two different facilities, one closed section facility for accurate aerodynamic measurements and one open-jet acoustic facility for noise measurements in good conditions of low background noise and anechoicity.

This is actually acceptable only if the flows are identical (or very close) in both windtunnels, which has to be carefully checked, experimentally and/or numerically. This assumption is generally reasonably true for non-lifting models (landing gear, cavity) of small overall dimensions compared to the dimensions of the test section (small blockage effect). On the contrary, lifting models (simple or high lift airfoil, full aircraft) always induce significant aerodynamic installation effects in open jet facilities.

3.4 Conclusions

As in many (not to say all) other scientific domains, it is nearly impossible to design a perfect aeroacoustic experiment for the validation of aircraft noise numerical prediction, simply because any test set-up has inherent drawbacks due to either aerodynamic or acoustic installation effects.

However, it is actually possible to propose a hierarchy, in terms of experimental difficulties, of aeroacoustic characterization of aircraft components. For example, engine components such as propeller, fan and jet noise sources are actually physically complex, but they are also efficient sources that can be designed in order to dominate the background noise of the facility, which makes them good candidates for acoustic characterization, including installation effects such as shielding by airframe surfaces. On the contrary, airframe noise sources are typically less efficient and more subject to the background noise and installation issues.

In the following of the lecture we give several examples of past projects in which most of these questions have been raised, sometimes remaining partially unanswered, definitely showing that the design of a validation experiment in aeroacoustics always relies on compromises.

4. LECTURE OUTLINE

This document is organized as follows.

In Section 5, we describe the main characteristics of aerodynamic and acoustic facilities that are cited in the examples.

In Section 6 we give several examples of aerodynamic installation effects, either in closed section facilities or in open section windtunnels. Then Section 7 describes situations where acoustic installation effects were assumed as critical in open test section windtunnels.

Finally Section 8 proposes a non-exhaustive list of experimental databases dedicated to the validation of aircraft noise computations, in the domains of airframe noise and fan noise, some of them being already public and others subject to an agreement with their respective owners.

5. WINDTUNNELS PRESENTATION

5.1 Aerodynamic closed section WT F2 (Onera)

Many examples in this lecture refer to measurements achieved in Onera's F2 facility operated at Onera-Le Fauga, near Toulouse (France). This closed-circuit facility, mainly used for internal Onera's research activities, has a test section of area 1.4 m x 1.8 m and a length of 5 m. The flow is generated by a 12 fixed bladed fan run by a 680 kW direct current motor, allowing flow velocity from 0 to 100 m/s. The specificity of F2 is that it has been designed for easy optical aerodynamic measurements, originally 2D and 3D LDV and now completed with 2D and 3D PIV. For this purpose, the optical instruments (emission and reception) are mounted on a massive framework support that can be moved in three directions and the lateral glass walls are transparent (Figure 3).

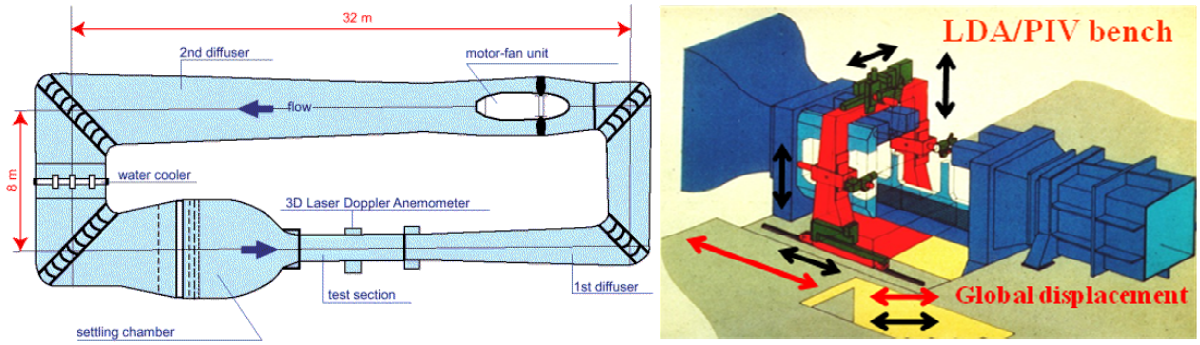

Figure 3 - Onera's F2 windtunnel

5.2 Acoustic open jet windtunnels

5.2.1 : CEPRA19 (Onera)

CEPRA19 is an industrial aeroacoustic facility operated by Onera in Saclay near Paris (France). It has been designed in the 70s for research on jet noise, and has been intensively used for engine (jet/fan) noise, including engine installation effects, and still presents interesting capacities for airframe noise measurements. It is mainly an anechoic room with a quarter-sphere shape of radius 9.4 m. The anechoicity is better than 99 % in the range [0.2 – 80] kHz. This room is traversed along the sphere diameter by an open circular jet generated by a nozzle of diameter either 2 m (with maximum velocity 130 m/s) or 3 m (with maximum velocity 60 m/s). Basic acoustic instrumentation relies on 2 circular arcs of 12 microphones each, in flyover (horizontal plane) and sideline (at 53° from the horizontal plane) directions. Additional acoustic measurements can be provided using various types of microphone antennas for noise source localization and ranking.

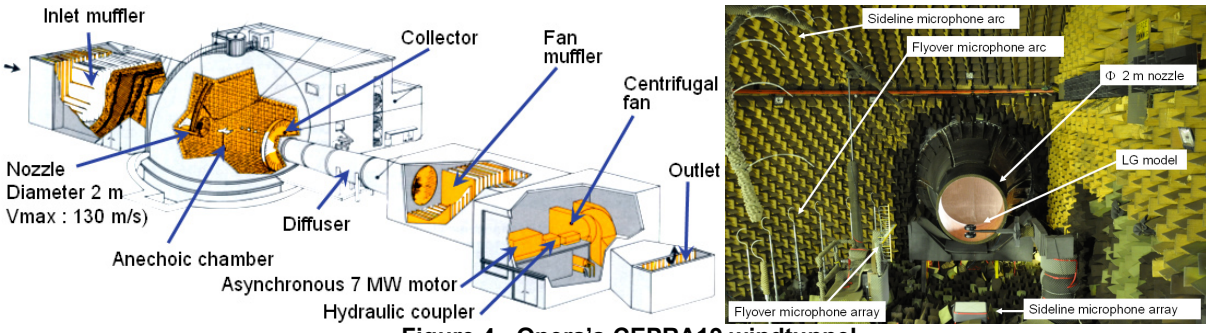

Figure 4 - Onera's CEPRA19 windtunnel

Aerodynamic measurements are possible, but limited and complex due to the location of the test section axis at about 4 m above the floor. A 2D/3D PIV system can be mounted on a specific support circling the open jet. A mobile probe support can be used to traversing measurements with any kind of Pitot and

hotwire probes. LDV is not available is this windtunnel (Figure 4).

5.2.2 Acoustics Centre Windtunnel (ECL)

The Acoustics Centre at Ecole Centrale de Lyon (France) operates a laboratory open-jet anechoic wind-tunnel which consists in a large anechoic room with height of 8 m and a floor surface of 10 m by 8 m. Typical nozzle of section 0.3 m high by 0.4 m wide generated flow up to 100 m/s (Figure 5).

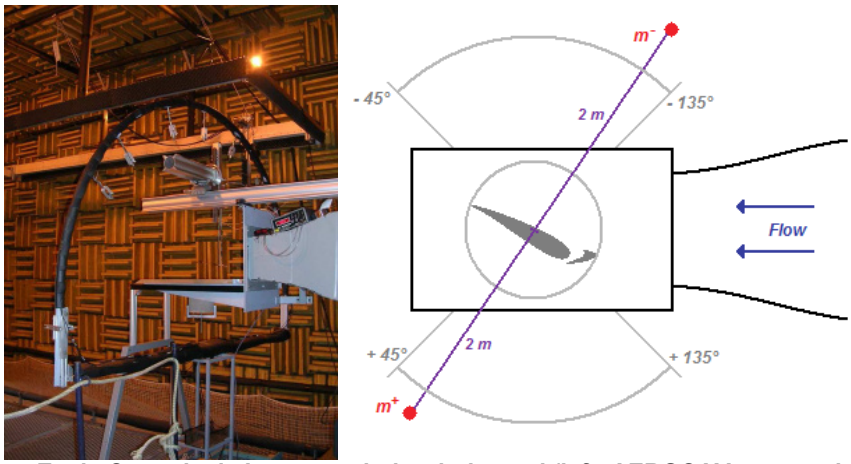

Figure 5- Ecole Centrale de Lyon anechoic windtunnel (left :AEROCAV set-up with cavity, right : VALIANT set up with slat/wing configuration)

A large door in the opposite wall allows the flow to escape the room. The cut-off frequency is about 80 Hz, and the measured background noise when the flow supply is off is around 21 dBA.

6. EXAMPLES OF AERODYNAMIC INSTALLATION EFFECTS

6.1 Simple airfoil (EXAVAC project)

In this internal project, Onera aimed at collecting an experimental aerodynamic and acoustic database on a two-dimensional NACA0012 model with a chord of 0.5 m and a span of 1.4 m. The objective was to combine aerodynamic tests in F2, with the model mounted between the lateral transparent walls, and acoustic tests in CEPRA19, with the model mounted between two large end plates that were designed to minimize the three dimensionality of the mean flow around the airfoil [2] (Figure 6).

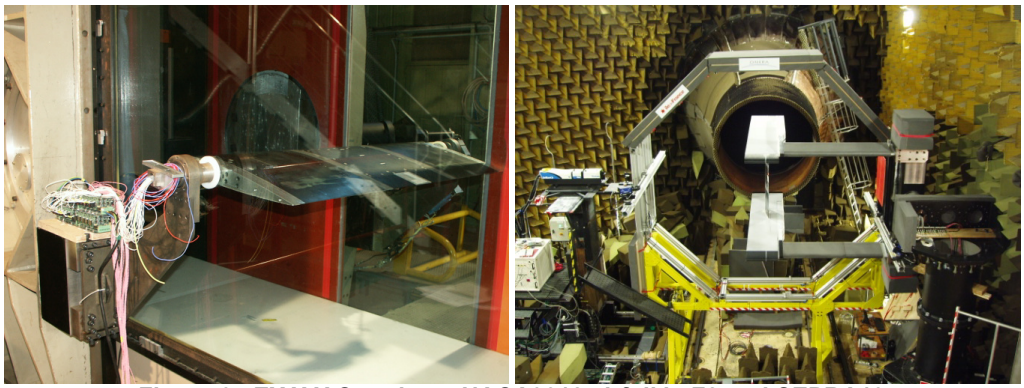

Figure 6 - EXAVAC project : NACA0012 airfoil in F2 and CEPRA19

A low incidence of 2.5° was chosen as a reference. The first issue was to compare the mean flows in both windtunnels for the airfoil at this reference incidence by using a section of static pressure probes at mid span of the airfoil. This comparison showed that the C_p reached much lower values in CEPRA19 than in F2, and it was necessary to increase the incidence up to 4° in the open-jet windtunnel to correctly match

the pressure distribution measured at 2.5° in the closed section wind tunnel (Figure 7).

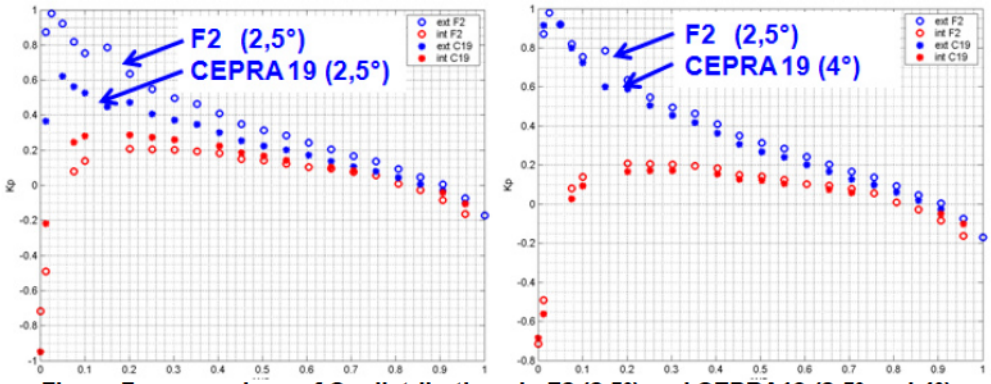

Figure 7 - comparison of Cp distributions in F2 (2.5°) and CEPRA19 (2.5° and 4°)

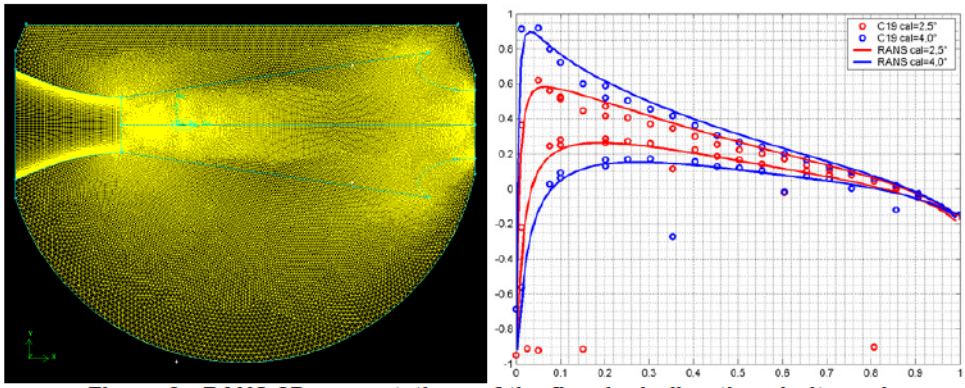

Figure 8 - RANS 2D computations of the flow including the windtunnel

In order to confirm that this anomaly was due to the different inflow conditions in both windtunnels, 2D RANS computations of the flow around the airfoil at several incidences were achieved, including the CEPRA19 flow topology, with an open jet generated by a nozzle and captured by a collector. Despite the 2D simplification of the computation with respect to the fully 3D experimental set-up situation, the computed Cp at 2.5° and 4° are in good agreement with the experimental data (Figure 8).

The conclusion was that, in an open-jet windtunnel, the flow around a lifting airfoil can significantly differ from the flow in free field or in a closed windtunnel, even if the airfoil lift is rather low (the lift coefficient was about 0.5 in this case). The problem can be obviously minimized by using a small model (with respect to the open flow section) but with the additional drawback of decreasing the aerodynamic noise generated by this model, with the possibility that this noise becomes masked by the background noise.

6.2 High lift wing with 2 elements slat-wing (TIMPAN and VALIANT projects)

6.2.1 TIMPAN

These aerodynamic effects can be even more pronounced with airfoils equipped with high lift devices. In the TIMPAN European project, Onera's global objective was to evaluate the potential of specific devices for slat noise reduction. The experimental approach relied on measuring deltas (no absolute levels) between several devices tested on the EUROPIV (RA16) model blown in CEPRA19 (Figure 8, left side). This 3-element (slat/wing/flap) airfoil has a significant chord of about 0.5 m and a span of 1.5 m. Even at low incidences (0° - 2°), and with the slat and flap deployed at 30°, this large airfoil generates a considerable lift. In order to minimize this lift and, thus, limit the windtunnel jet deviation, the chosen approach was to evaluate a 2-element (slat, main wing and retracted flap) configuration which was assumed to:

- mimic the flow in the slat cove of the 3-element airfoil,
- minimize the total lift,

- minimize the flap and trailing edge noise sources (Figure 9, right side).

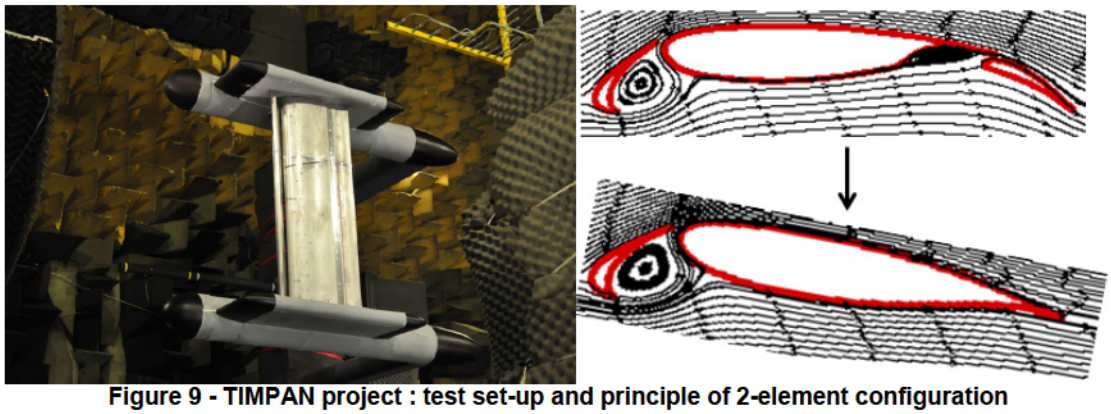

Figure 9 - TIMPAN project : test set-up and principle of 2-element configuration

This preliminary study was achieved by using 2D RANS computations of both 2- and 3-elements configurations at various incidences. The identification of the mean flows in the slat cove region was roughly assumed in two ways, (i) visual comparison of stream lines and (ii) numerical comparison of Cp distributions in the slat cove. For example, the flow in the slat cove of the 3-element airfoil at an incidence of 0° (resp. 2°) was found approximately identical to the flow in the slat cove of the 2-element airfoil at an incidence of 9.5° (resp. 11.5°). Moreover, the examination of the polar aerodynamic laws (lift coefficient function of the incidence) showed that the lift coefficient of the 3-element at 0° (resp. 2°) was about 2.6 (resp. 2.8) whereas it was less than 1.6 (resp. 1.7) for the 2-elements at 9.5° (resp. 11.5°) (Figure 10).
In addition, RANS 3D computations of the full airfoil with its support were achieved including the whole windtunnel configuration (test room, nozzle and collector), showing that, even with this minimized lift, the 2-element airfoil induced a very strong deviation of the windtunnel flow on the collector, an aerodynamic effect which is evidently accompanied by a strong increase of the windtunnel background noise.

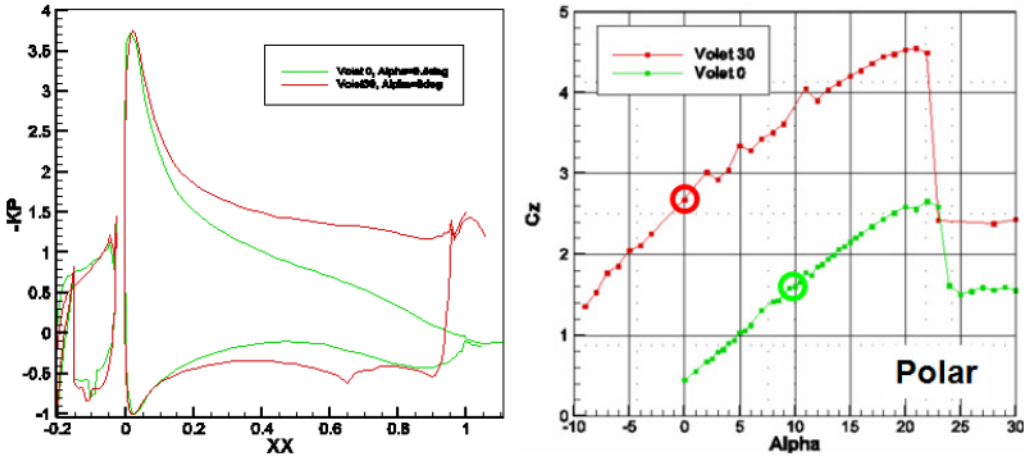

Figure 10 - Left: comparison of Cp for 3-element at incidence 0° and 2-element at incidence 9.5°. Right: polar for 3-element and 2-element configurations

6.2.2 VALIANT

In the "Airfoil with slat" task of the VALIANT European project, ECL's and Onera's common objective was to build an aerodynamic and aeroacoustic experimental database for the evaluation and validation of slat flow/noise numerical predictions methods. The chosen approach was to achieve these tests in ECL's acoustic windtunnel, in parallel of a similar joint activity on flap noise, by using a model specifically designed and manufactured for this purpose. This was achieved under the following constraints:

- The mechanisms involved in slat noise generation are very specific, so it was critical to generate a flow with steady and unsteady features as close as possible to the flow in the slat cove of a realistic

high lift wing.

- ECL's facility has a modest test section of 0.3 x 0.4 square meters, which means that any lifting model of significant size immediately induces a strong deviation of the windtunnel open jet, with a corresponding degradation of the mean flow conditions compared to free field. Consequently, it was even more critical to minimize the model lift in this case.
- Finally, since only slat noise was aimed at, it was desirable to get rid of any unrelated noise source such as flap or trailing edge noise sources.

The chosen approach was to adapt an existing 3-element (slat/wing/flap) airfoil (Airbus FNG airfoil with a retracted chord of 0.3 m and a reference global incidence of 6°) and transform it into a 2-element airfoil (slat and main element, flap suppressed), with the (upstream) slat cove region unchanged, and the (downstream) shape (wing TE) adapted. Unlike the precedent TIMPAN case, this adaptation was achieved through a systematic numerical optimisation process using optimization software (DAKOTA - Sandia Labs) through 2D RANS computations (*elsA* solver) and automatic re-meshing. In this process, the two cost functions to minimize where (i) the global deflection of the mean flows and (ii) the difference between the mean flows in the slat cove of the 2- and the 3-elements airfoil. The two free parameters were (i) the airfoil global incidence θ and (ii) the vertical position of the sharp wing trailing edge y_{TE}. The process led to optimal values of $\theta = 18°$ and $y_{TE}/C = 0.06$ (Figure 11) [3].

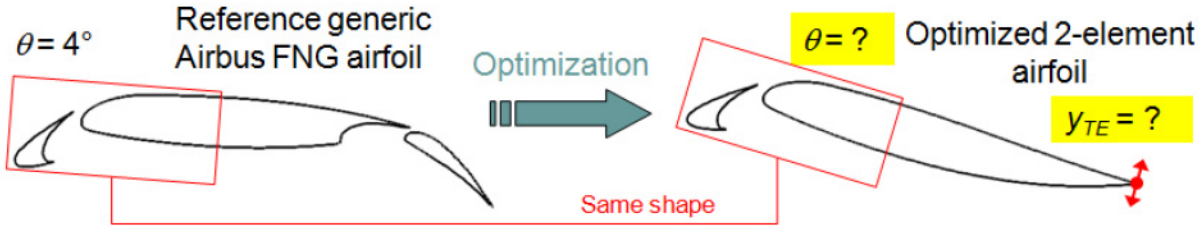

Figure 11 - Optimization of the VALIANT 2-element (slat/wing) configuration → optimal configuration θ = 18° and yTE/C = 0.06

With these optimal parameters, the mean flow in the slat cove was very close to the original one (and it was assumed that the unsteady flow was also very similar), whereas the total lift of the 2-element model (at the incidence 18°) was reduced by more than 60 % with respect to the 3-element airfoil at the incidence of 6°, without generating an excessive flow separation at the wing trailing edge, which could have generated a strong unwanted noise source (Figure 12).

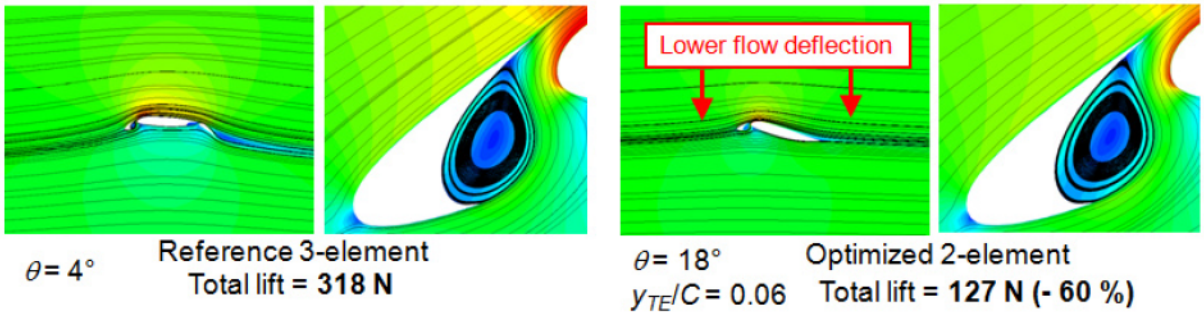

Figure 12 - VALIANT "Airfoil with slat": results of optimization : global lift reduction (RANS 2D)

However, this optimization was achieved for an airfoil in infinite or free-field conditions. Even with a reduced lift, the airfoil induced a significant flow deflection: when the model was mounted in the windtunnel, a final adjustment of the incidence had to be achieved, by comparing the *Cp* distribution measured in the mid-span section to the theoretical pressure distribution of the airfoil in free-field (Figure 13, left side).

This led to an optimal incidence of 25°. This surprising result was confirmed later by new 2D RANS computations which included the windtunnel open jet flow and nozzle, the latter being simply meshed using IBC (Immersed Boundary Conditions). Note that this IBC technology was not available when the

airfoil was designed, otherwise the optimization should have been directly achieved for the airfoil in open jet conditions (Figure 13, right side).

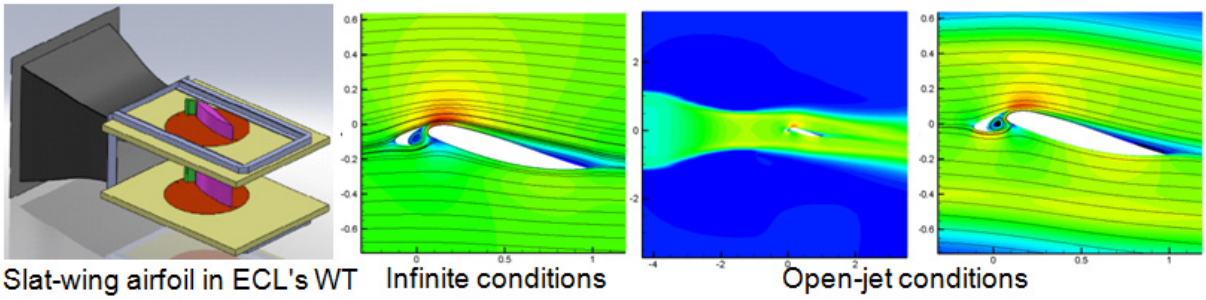

Figure 13 - Adaptation of VALIANT "airfoil with slat" in windtunnel : test set-up, flow in infinite and open-jet conditions at incidence 18°

6.2.3 Conclusions

A straightforward conclusion of the last three examples of testing lifting airfoils in open-jet windtunnels is that such experiments require to carefully evaluating the actual 3D flow conditions, because it is unlikely that these conditions will be identical, or even close, to the free-field conditions, unless the model is very small compared to the windtunnel section area. For this reason, such experiment can be used only to validate aeroacoustic prediction in which the flow computation accounts for the open jet flow conditions.

6.3 Landing gear (LAGOON project)

The next example shows that the exercise is easier in the case of a non-lifting model. In the LAGOON project, Airbus's and Onera's common objective (along with DLR and Southampton University) was to build an aerodynamic and aeroacoustic experimental database for the evaluation and validation of landing gear flow/noise numerical predictions methods [4]. The chosen approach was to use a very simplified 2-wheel landing gear model in two successive facilities, first in the F2 facility for accurate aerodynamic measurements, then in the CEPRA19 windtunnel for acoustic measurements. The model presents a perfect lateral symmetry and an asymmetry in the vertical direction due to the main leg, which induces a weak lift. Consequently the only expected differences between the mean flows in both windtunnels could only derive from different blockage coefficients (the latter was estimated to be less than 6 % in the F2 test section).

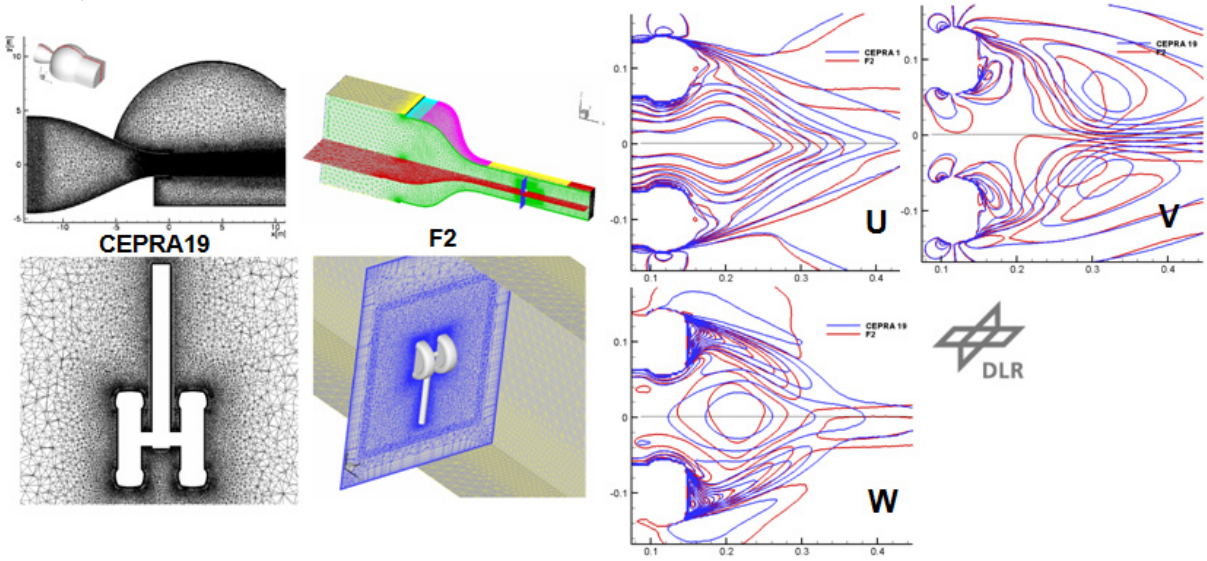

Figure 14 - LAGOON simplified 2-wheel landing gear : RANS 3D including aerodynamic installation in F2 and CEPRA19 (achieved by DLR with TAU)

From the start, an assumption of identical flows was made, which had to be checked in two ways.

The first approach was to conduct three dimensional RANS computations of the flow around the model in both windtunnel, including the open-jet conditions and nozzle in CEPRA19, a task that was achieved by DLR with the solver TAU (Figure 14) [5].

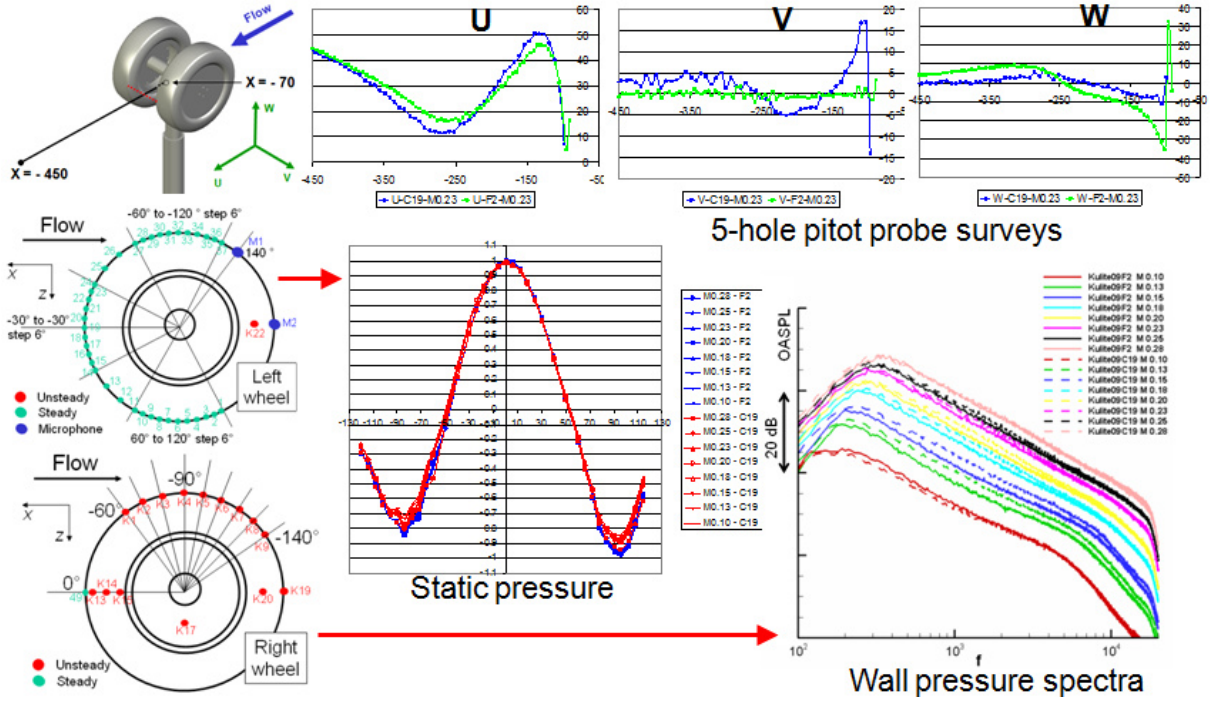

Figure 15 - LAGOON simplified 2-wheel landing gear: comparisons of static wall pressure coefficients distributions, unsteady wall pressure spectra, and (limited) velocity flow surveys using a 5-hole Pitot probe in F2 and CEPRA19

The second assessment was experimental, relying on comparisons of the static wall pressure coefficients distributions, unsteady wall pressure spectra, and (limited) velocity flow surveys using a 5-hole Pitot probe in both windtunnels (Figure 15).
These two assessments showed very tiny differences, which were actually attributed to a larger blockage effect in the closed section windtunnel, which locally induced larger velocities in the confined situation. These differences were too tiny to justify any systematic correction.

6.4 Cavity (AEROCAV project)

However, the next example shows that, even when the studied model is not supposed to induce any strong aerodynamic loads, it can be tricky to identify mean flows for a given configuration tested in two different facilities. In the AEROCAV (*AEROacoustics of cylindrical CAVities*) French project, ECL's and Onera's common objective (with Airbus and several French academic partners) was to build an aerodynamic and aeroacoustic experimental database for the evaluation and validation of numerical predictions methods for the unsteady flow and noise of a cylindrical cavity of diameter and depth equal to 0.1 m [6]. Such cavities are present on fuselage and wings of transport aircraft, and are known to generate tonal noise. The chosen approach was to test the same cavity, manufactured by ECL and fully equipped with static wall pressure taps and unsteady pressure sensors, firstly in ECL's aeroacoustic windtunnel for acoustic measurements (and also limited aerodynamic measurements), then in Onera's F2 windtunnel for accurate aerodynamic measurements, including simultaneous 2-point velocity acquisitions using 3D LDV and a hotwire probe.
In this case, the critical issue for the F2 tests was to feed the cavity with the same mean upstream flow as in ECL's windtunnel, in which the velocity profile and boundary layer thickness upstream the cavity had been accurately measured. For this purpose, it was decided to use a "fake" floor in F2, placed 30 cm above the test section floor. Then velocity profiles were measured on this "fake" floor at several axial positions and, after selecting the position which offered the best match with measurements at ECL, the floor was

drilled and the cavity was mounted at the (expected) best place. Unfortunately, when the velocity profile was checked after mounting the cavity, it was found to strongly differ from the profile measured without the cavity at the same position. Unfortunately, the cavity could not be moved any more (Figure 16).
Rapid investigations supported by 2D RANS computations of the flow in the median test section, showed that the beveled leading edge of the "fake" floor was very sensitive to any modification of the flow below the floor, and the insertion of the cavity model was actually a critical modification (Figure 17).

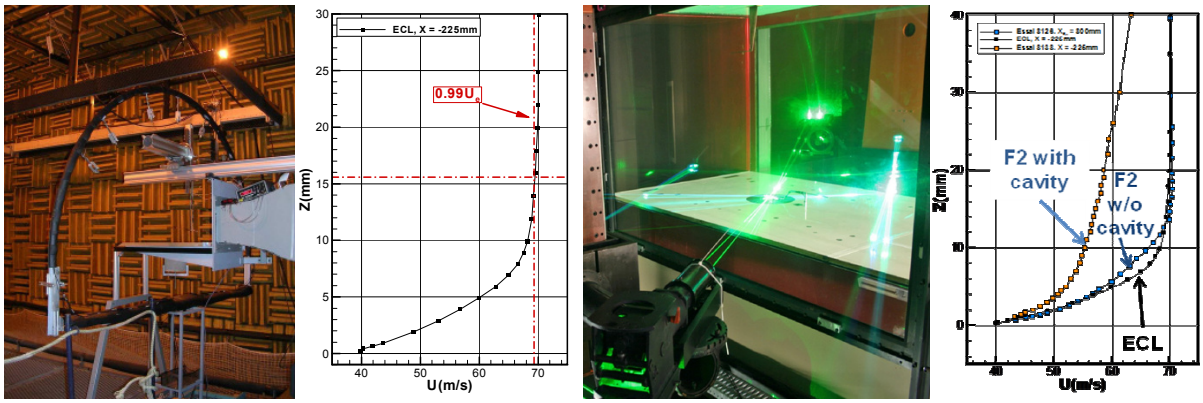

Figure 16 - AEROCAV. From left to right :test-set-up and velocity profile upstream the cavity in ECL's acoustic windtunnel, test set-up and velocity profiles in Onera's F2 aerodynamic windtunnel, before and after mounting the cavity on the floor

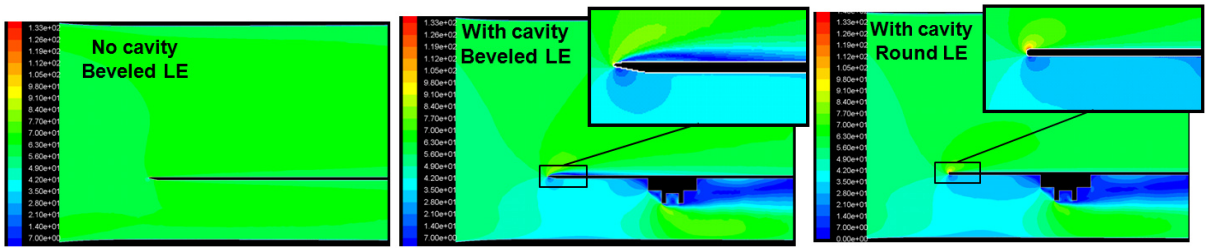

Figure 17 - AEROCAV. 2D RANS computation of the mean flow on the "fake" floor with beveled or rounded leading edge, without and with the cavity model

Several leading edge shapes were numerically tested and it was found that the most insensitive to underneath flow change was a simple circular leading edge. A final adjustment of the boundary layer thickness on the floor was obtained by tripping the laminar-to-turbulent transition using a "zig-zag" adhesive tape at a selected position. Finally there was still a lateral (Y) asymmetry of the velocity profile at the X position of the cavity, which was simply due to the asymmetry of the thick wire harness that led the wires and pipes from the cavity to the windtunnel floor. This was easily corrected by using a vertical pipe to home this wire harness. The conclusion is that there are no straightforward set-ups in aerodynamic test.

6.5 Simple jet

Aerodynamic effects may also have significant influence on the aeroacoustic characterization of engine noise sources such as a simple jet, as depicted on Figure 18, which compares unsteady flow prediction of an isolated simple jet (diameter 80 mm) computed with Onera's unstructured solver CEDRE (LES method), and farfield noise extrapolation using Onera's FW-H solver KIM, with jet noise measurements achieved in Cepra19.
This study demonstrates a classical bias of jet numerical predictions with respect to experimental data. In the experiment, there is natural initial turbulence in the nozzle, which is typically omitted in numerical simulation, in which the initial flow is laminar, so the laminar-turbulent transition which occurs downstream generates additional noise. This bias is suppressed when the numerical simulation uses a more resolved grid and includes a turbulence tripping device inside the nozzle [7].

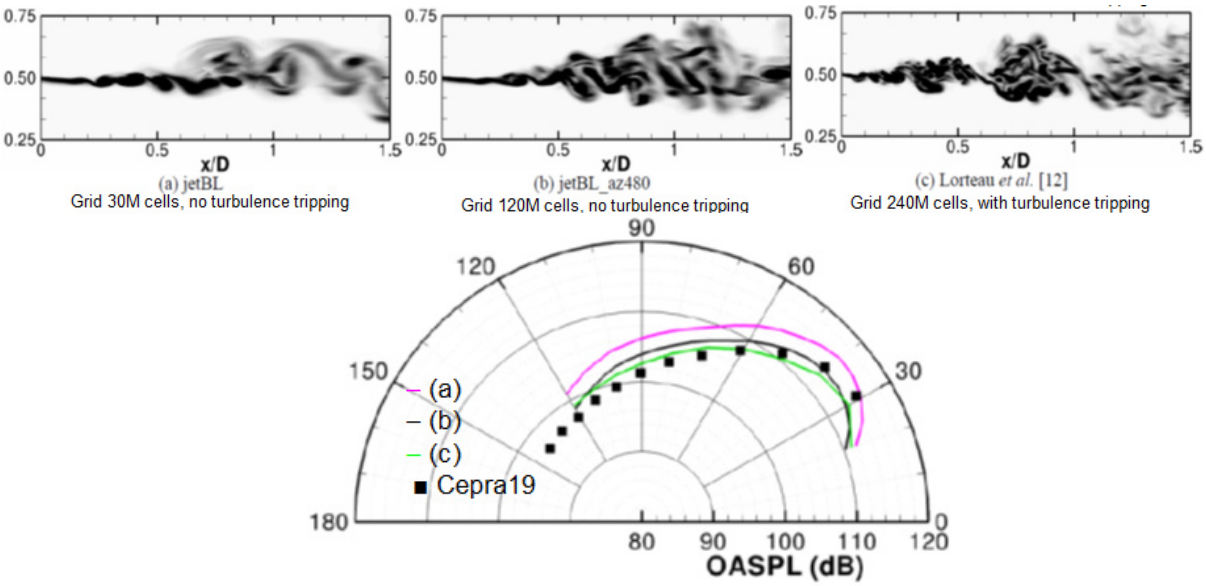

Figure 18 - Aerodynamic installation effects on isolated simple jet

6.6 Fan noise installation effects

The next example illustrates the difficulty to correlate a numerical simulation with a complex experiment of aft fan noise installation effects. In the EC project NACRE (Novel Aircraft Concepts Research in Europe), innovative engine installation were studied in Cepra19 with the objective of characterizing engine noise shielding by the airframe elements, for example the U-tail that can be seen on Figure 19 (top left). The experiment combined a generic Airbus aircraft model and a fan noise simulator (TPS - Turbine Power Simulator), with several relative positions. The far field noise was measured with a transverse circular antenna of microphones of diameter 6 m that could be moved in the flow direction, thus covering a circular cylinder around the aircraft. The TPS is an actual fan/OGV operating in a realistic nacelle equipped with a circular array of pressure sensors to characterize the modal content of the aft fan noise radiated through the nozzle.

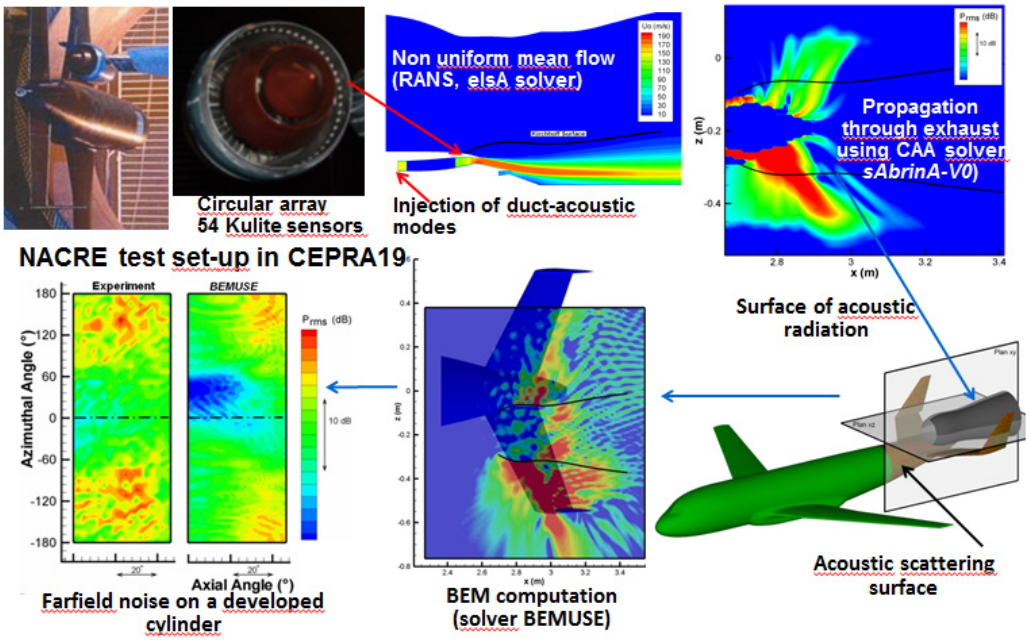

Figure 19 - Aerodynamic/acoustic installation effect on fan noise using CAA/BEM

In the numerical simulation, this modal acoustic field was injected inside the isolated nacelle in a CAA computation (*sAbrinA.v0* solver) accounting for the strongly inhomogeneous mean flow obtained with a RANS method (*elsA* solver). This sound field was extracted on an axisymmetrical control surface surrounding the nacelle. This pressure field was used to compute the incident sound field on the rear fuselage of the aircraft, then a boundary element method (BEM – *BEMUSE* solver) was used to compute the scattered and total acoustic fields [8].
The final comparison of the predicted and measured sound fields on a developed cylinder is shown on bottom-left of Figure 19. Azimuthal direction 0° corresponds to the flyover direction, where the shielding effect is maximal, whereas 90° and 270° correspond to sideline directions. The experimental tendencies are correctly recovered by the computation, but with several differences that can be explained by weaknesses of the BEM, such as the absence of convection and the partial inclusion of the airframe, limited to the rear fuselage and the U-tail for reasons of computational resources with respect to the frequency.

7. SPECIFICITIES OF ACOUSTIC INSTALLATION EFFECTS IN OPEN TEST SECTION

7.1 Corrections for acoustic refraction through jet shear layer

Open-jet windtunnels are generally the best choice for acoustic measurements because they can offer acoustic radiation conditions close to free-field (as long as the test chamber is large enough and equipped with anechoic or sound absorbent walls) and allow the acoustic detection of weak aeroacoustic sources (as long as the background noise is low enough). However, farfield noise instrumentation in such facilities is commonly located outside the flow, so the acoustic path between the inflow source(s) and the observer is never a straight line, due to the refraction effects through the jet shear layer. This has significant consequences in the context of the validation of numerical predictions of acoustic radiation, which generally assumes that the flow is uniform between the source and the observer. For a fair comparison, measurements must be corrected, which is generally done by providing the coordinates of an "equivalent observer in uniform flow" which provides the same acoustic path as in the refracted medium, in terms of length and phase shift. Then the noise predictions achieved at these equivalent observer positions are directly comparable to the measurements achieved at the physical positions (Figure 20).

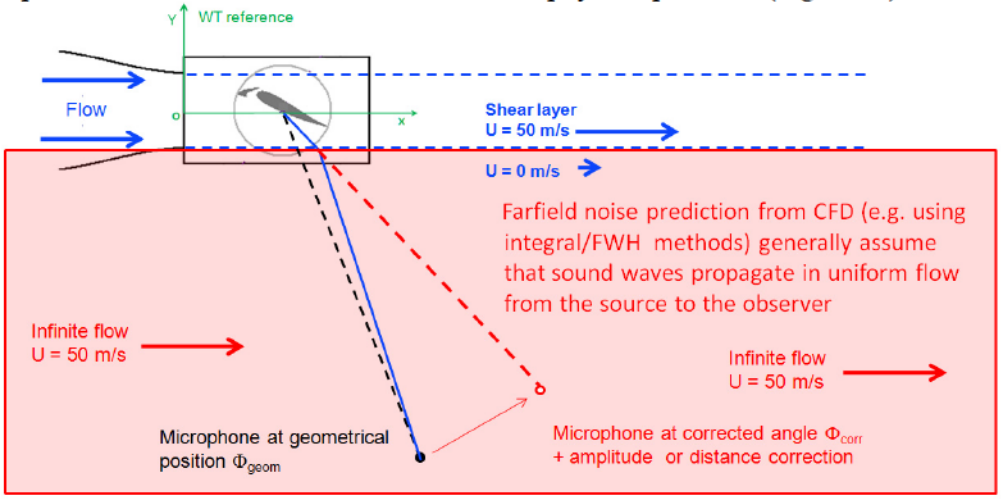

Figure 20 - Correction of acoustic refraction effects in open-jet acoustic windtunnel

There have been several models [9] [10] proposed to achieve this refraction correction, most of them assuming that:

- the open jet is perfectly cylindrical (circular or rectangular depending on the nozzle shape), or keeps a constant section in the axial direction (no expansion),
- the shear layer between the jet flow and the medium at rest has a zero or negligible thickness,

- the source is located at the jet centre line.

7.2 Validation of noise prediction from CFD on an airfoil with limited span

Due to the current limitations of CPU and memory resources of even the largest parallel computing clusters, unsteady CFD of (simple or high-lift) airfoil flows using LES-like methods (DES, ZDES, NLDE) are generally limited to 2.5D airfoils (with a constant section in the spanwise direction) and a computational domain with a limited span extent S_{CFD} (generally several percents of the airfoil chord), in association with a periodicity condition in this spanwise direction. Then, acoustic methods are used to evaluate the noise radiated in its median plane by this "slim" computational airfoil, with valuable qualitative information, for example in term of directivity diagram, but raising the question of comparison to acoustic measurements achieved with a 2.5D airfoil having the same section but much larger span S_{Exp} (the aspect ratio span/chord is always larger than 1, and preferably in the range 2-4).

A typical approach, proposed by several authors (but originally attributed to Kato [11]), is to "virtually" duplicate the computational domain N times (with N=S_{Exp}/S_{CFD}) in the spanwise direction and to consider that the summation of all N individual pressure contributions $p_i \left(i=1,...,N\right)$ radiated at the observer position is a good estimation of the acoustic pressure radiated by the experimental airfoil (Figure 20, left side). Following this assumption, the acoustic power at the observer position is written $p^2 = \sum_{i,j=1,N} p_i p_j^*$

where * denotes the complex conjugate. This simple result leads to two very different cases:

- If all N contributions are considered as fully de-correlated, then $i \neq j \Rightarrow p_i p_j^* = 0$, and $p^2 = \sum_{i=1,N} p_i^2$, which means that, if all N elements are assumed to radiate the same sound power $p_i^2 = p_{CFD}^2 \left(\forall\, i=1,N\right)$, then the estimation for the duplicated airfoil is $p^2 = N p_{CFD}^2$.
- If all N contributions are considered as fully correlated, and all N elements are assumed to radiate the same sound pressure $p_i^2 = p_{CFD}^2 \left(\forall\, i=1,N\right)$ then $p_i p_j^* = p_{CFD}^2 \left(\forall\, i,j\right)$ and $p^2 = N^2 p_{CFD}^2$.

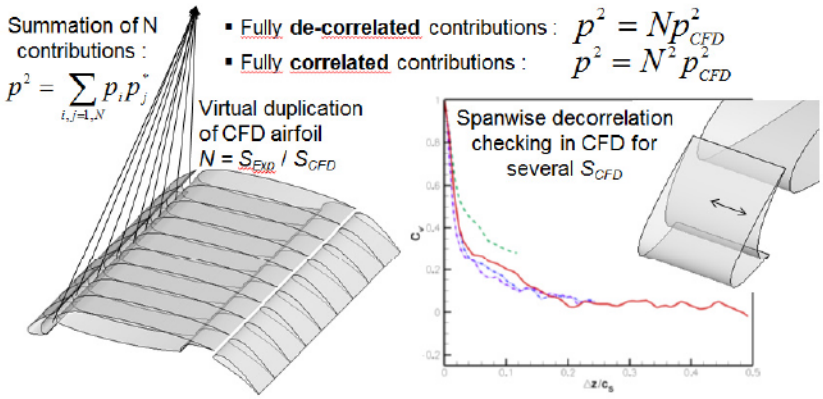

Figure 21 - Validation of noise prediction from CFD on an airfoil with limited span : virtual duplication of CFD airfoil and checking of spanwise decorrelation.

In the first case (de-correlated summation), the noise radiated by the full span airfoil (S_{Exp}) is estimated from the noise computed from the CFD domain (S_{CFD}) with a simple correction of (10 log N) decibels. In the second case (correlated summation) the required correction is (20 log N) decibels. For all intermediate cases of partial correlation, the correction lies between these two extreme values.

In most cases, the computational span S_{CFD} is large enough to ensure that the turbulent structures (or aeroacoustic sources) generated by the CFD in the computational domain have spanwise length scales smaller than S_{CFD}, which means that the cross-correlation of such structures between two points along the span distant of more than S_{CFD} is negligible and the first case applies. This de-correlation along the span can be checked experimentally (requires simultaneous 2-point velocity or pressure measurements) or directly from the results of unsteady CFD (Figure 20, right side).

7.3 The "signal to noise" ratio issue in open-jet acoustic windtunnel ("de-noising" technique)

7.3.1 Introduction

An important issue of acoustic measurements in an anechoic silent windtunnel is the "signal to noise" ratio or the difference (in decibels) between (i) the noise radiated by the model itself and (ii) the background noise level measured, for example, without any model mounted in the windtunnel. When using simple microphone instrumentation, it is necessary that this ratio remains larger than a given value, generally chosen at about 3 dB, in order to avoid that the measurement is affected by the background noise.

7.3.2 Simple airfoil (EXAVAC project)

If we go back to Onera's internal project EXAVAC, a two-dimensional NACA0012 model with a chord of 0.5 m and a span of 1.4 m was tested in CEPRA19 (Figure 6, right side), again to collect data for the validation of numerical methods for the prediction trailing edge noise [2]. In order to ensure that the flow around the airfoil was as close as possible to a two-dimensional flow, the airfoil was mounted between two large end-plates covered with absorbing foam to minimize reflections (Figure 22, top left). The airfoil had a blunted trailing edge which was supposed to generate a vortex shedding with a resulting tone noise at an identified frequency near 2.8 kHz. Unfortunately, it was found that the farfield microphones mounted in the anechoic chamber at a distance of 6 m from the airfoil were unable to detect this tone (Figure 22, top right).

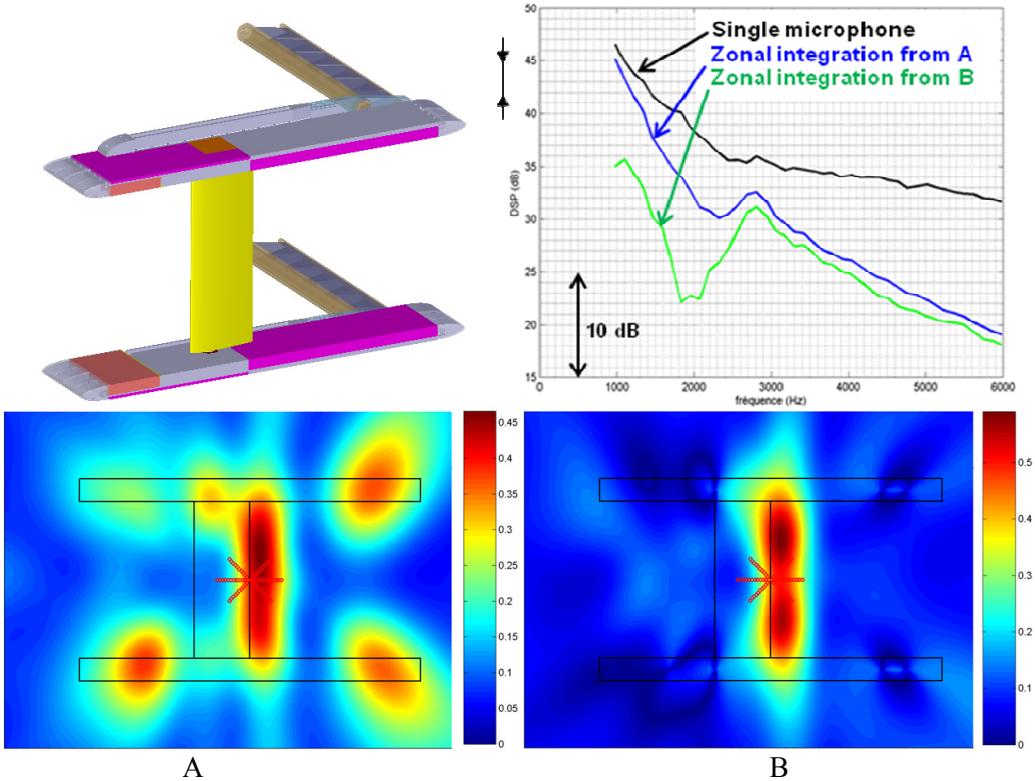

Figure 22 - EXAVAC project (NACA0012 airfoil in CEPRA19). Test set-up and farfield noise spectra measured by a single microphone (black) and zonal integrations from beamforming maps A (classic, blue) and B (advanced, green).

Examinations of noise maps generated using classic beamforming from a microphone antenna clearly showed that there were unwanted noise sources located on the end plates, sources that were expected to mask the (weak) trailing edge noise source.

A zonal integration in the trailing edge region of these noise maps at any frequency of interest provided the airfoil trailing edge noise spectrum with its characteristic tonal source. Additionally, an advanced

beamforming method was used, based on adaptive filtering of the spurious noise sources (zeroing the side lobes of the beam forming filter at the positions of the sources, which were detected by classical beamforming). With this advanced process the contributions of the spurious noises sources to the tonal component were eliminated (Figure 18).
This example shows that, in open-jet windtunnel, the use of a microphone antenna with advanced beamforming processing associated with zonal integration of noise maps, can compensate a problem of low signal-to-noise ratio. This is also possible in closed section windtunnels but with additional issues due to confinement and the presence of image-sources outside the test section, generated by reflections on hard walls.

7.3.3 High lift airfoil (Airfoil with slat) VALIANT project

In the second example of the configuration « Airfoil with slat » of the VALIANT project, already presented before (Figure 11 to Figure 13), the beamforming with a microphone antenna of 120 microphones was used to demonstrate that no spurious noise sources were present and that the signal-to-noise ratio was sufficient. Indeed, on noise maps computed at several frequencies, it can be observed that the main noise sources are actually located in the slat region (Figure 23). The important result in this case is that no other significant sources are detected in the region concerned by the beamforming, especially at the trailing edge of the end plates. This is an important result in the context of validation of numerical methods, since it ensures that the farfield noise levels measured in the windtunnel are actually generated by the slat region, so they can be compared to slat noise prediction with confidence.

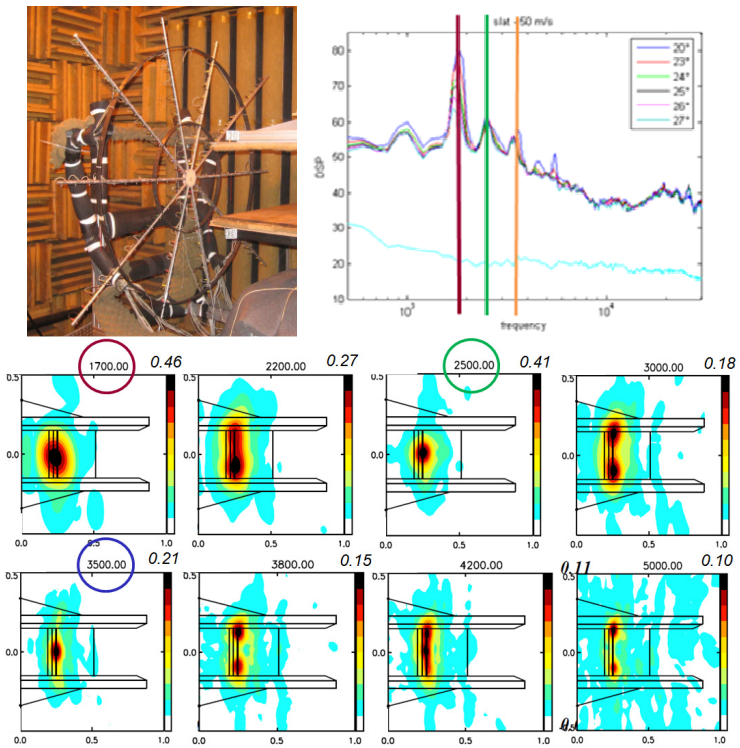

Figure 23 - VALIANT airfoil with slat. Onera's microphone antenna. Typical noise spectra measured by one microphone. Noise maps at several frequencies

Moreover these noise maps showed the qualitative result that, at the frequencies of the tones, the noise sources were preferably found along the slat region and, at intermediate frequencies, the sources were preferably located near at the junction between the slat and the end-plates holding the model (Figure 23). This was confirmed by additional beamforming based on DAMAS process from which spectra of noise generated by various regions of the airfoil were obtained by integration of the noise maps (Figure 24). It is interesting to see that the noise spectrum generated by integration of the full airfoil surface is very close to the spectrum measured by a single microphone [12].

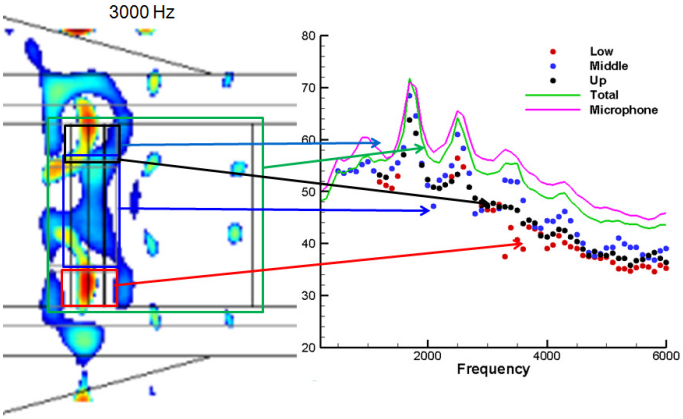

Figure 24 - VALIANT airfoil with slat. Noise maps from DAMAS beamforming process. Noise spectra from zonal integration on several regions

7.4 The "signal to noise" ratio and confinement issues in closed section windtunnel ("de-confinement" and "de-noising" techniques)

7.4.1 High lift wing noise measurements in closed section windtunnel

In this section we show results of acoustic measurements of a 3-element high lift wing (DLR's F16 or LEISA2 airfoil) in Onera's F2 closed section windtunnel and DLR's AWB anechoic silent open-jet facility. This two-dimensional model has a retracted chord of 300 mm and different spans in AWB (0.8 m) and F2 (1.4 m). In both experiments, microphone arrays were used for noise characterization in the flyover direction (Figure 25).

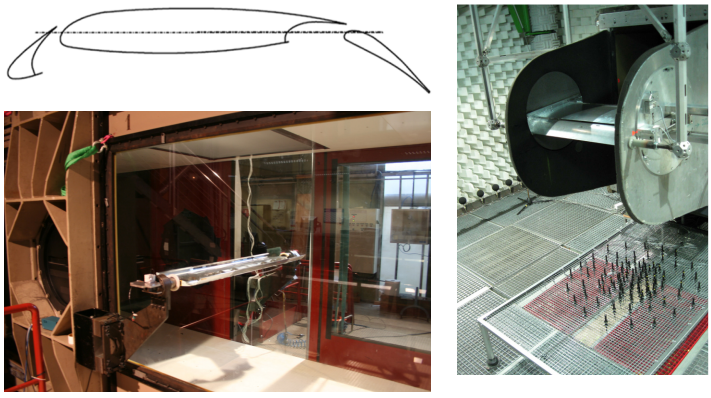

Figure 25 - Top left : LEISA2 (F16) airfoil section. Model in F2 (left) and AWB (right)

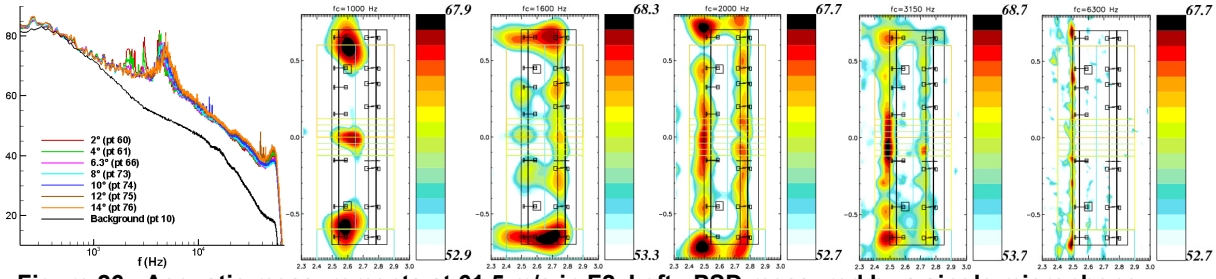

Figure 26 : Acoustic measurements at 61.5 m/s in F2. Left : PSD measured by a single microphone : background noise and model at various incidences. Right : DAMAS noise maps at incidence 6.4° and frequencies 1, 1.6, 2, 3.15, 6.3 kHz. Flow direction is from left to right.

Figure 26 shows acoustic measurements at 61.5 m/s in F2. Left plot shows power spectral densities measured by a single microphone (i) with the model at various incidences, and (ii) without the model (background noise). Right plots show DAMAS noise maps measured at an incidence of 6.4° and for

several frequencies. The flap is the main source below 2 kHz, whereas the slat dominates at higher frequencies. This is confirmed on Figure 27, where spectra derived from the integration of noise maps in various areas are compared. Note that the integration of the total scan area closely match the single microphone measurement, showing that no other noise source significantly influences the measurement in this frequency domain (above 500 Hz).

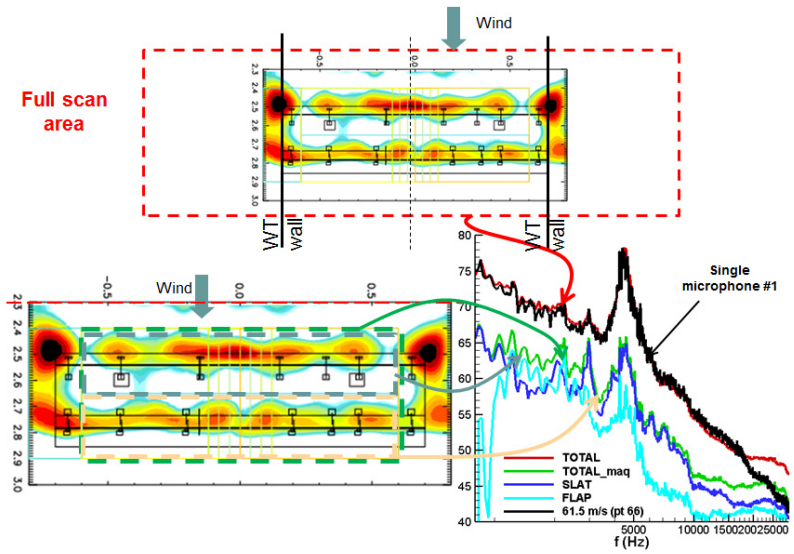

Figure 27 - PSDs from noise maps (DAMAS) integration on various areas

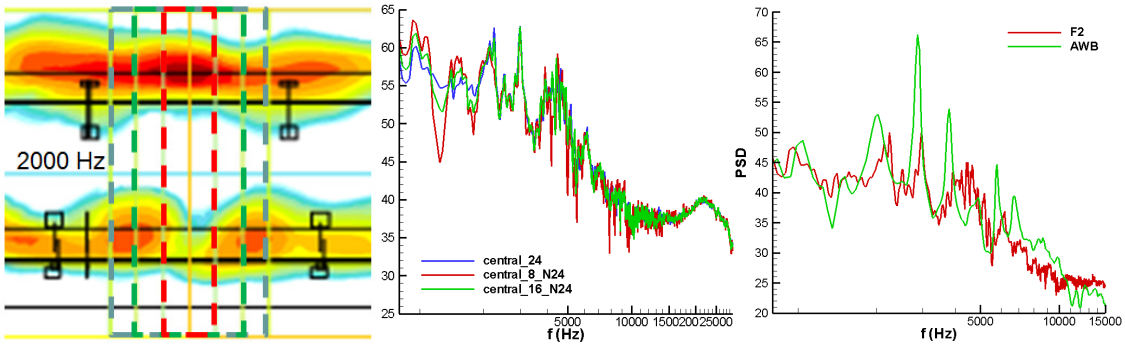

Figure 28 : PSDs from noise maps (DAMAS) integration on central sections of span 8, 16 and 24 cm, normalized by the span (left and centre). Comparison with similar measurements in the anechoic open-jet windtunnel AWB (DLR)

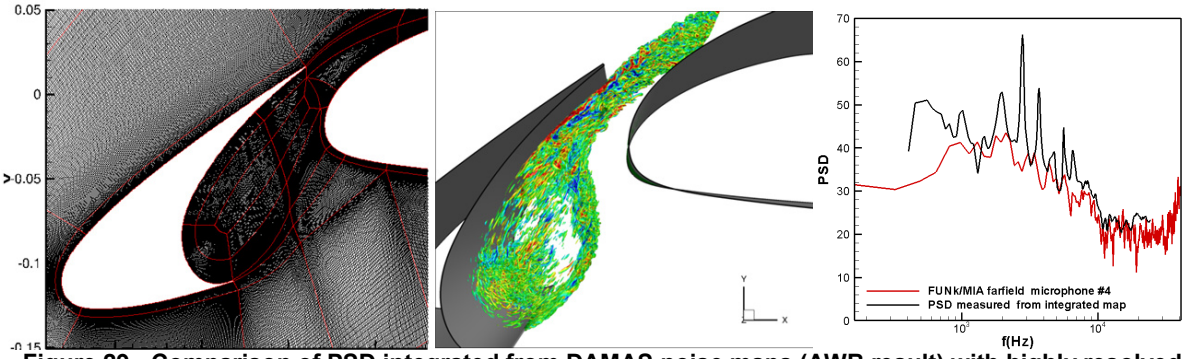

Figure 29 - Comparison of PSD integrated from DAMAS noise maps (AWB result) with highly resolved LES (FUNk solver) – All levels normalized to the same span of 24 cm.

Finally, Figure 28 shows similar results for the 3 central sections of the airfoil (span 8, 16 and 24 cm) shown on the left plot. On the central plot the PSD integrated from the DAMAS noise maps in these three areas are normalized by their individual span. The collapse of the normalized PSD indicates that the noise

sources are fully decorrelated in the span direction. The right side plot shows a comparison with similar measurements in the anechoic open-jet windtunnel AWB (DLR). The broadband continuum of the spectra are very close, but AWB result displays tonal components at slightly different frequencies and much higher levels [13].
Despite these differences, such result is a good candidate for the validation of numerical simulations. Figure 29 shows comparison of the PSD integrated from DAMAS noise maps measured in AWB, with a result derived from a highly resolved LES computation (Onera's FUNk solver), and the far field noise computed with a FW-H integration (MIA solver) [14]. Note that all noise levels (experimental/numerical) are normalized to the same span of 24 cm. The broadband levels are in good agreement, but the computation does not reproduce the strong tonal peaks, that are specific of the AWB installation.

7.4.2 Experimental validation of the "de-confinement" and "de-noising" method

The results presented in the last section show that, using a microphone array and adequate signal processing techniques, it is possible to characterize the noise generated by a given region of the model, with no significant influence of the background noise and the image-sources generated by acoustic reflections on the hard walls. Such result is of primary importance for further validation of aeroacoustic numerical simulations.
In this section, the objective is to confirm this result through a more basic experiment in the same F2 windtunnel equipped with the same microphone antenna. For this purpose we use a circular cylinder bar of diameter 70 mm mounted "wall-to-wall" in the windtunnel, with two possible sweep angles of 0° and 30°. The lateral walls of the windtunnel are either rigid or equipped with absorbent liners (Figure 30).

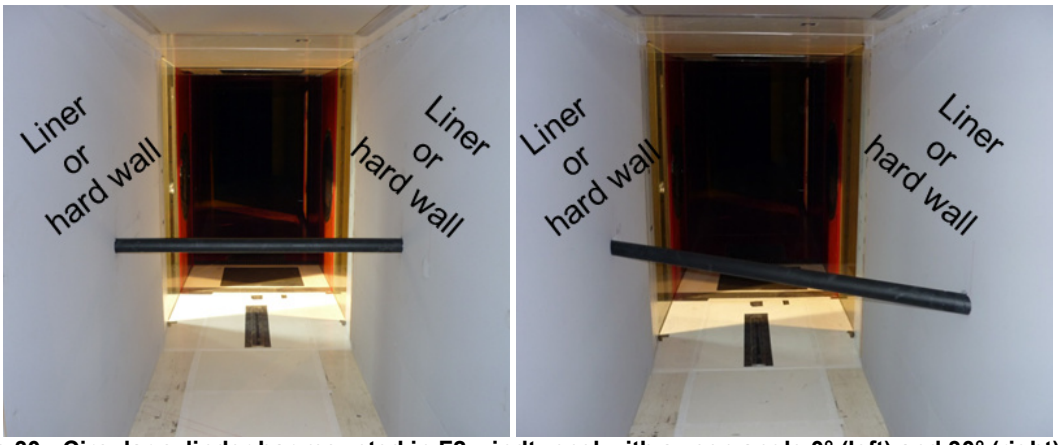

Figure 30 - Circular cylinder bar mounted in F2 windtunnel with sweep angle 0° (left) and 30° (right), with lateral walls either rigid or equipped with absorbing liners

For flow velocities in the range 40-80 m/s, such cylinder generates a broadband noise with a uniform distribution of noise sources in the span direction. Figure 31 (left) shows two scan areas used for acoustic beamforming. The small area is limited to the region inside the test section, whereas the larger area extends outside this test section. On the right side of Figure 31, are displayed the noise maps obtained for both scan areas, in the hard wall configuration, for the straight and swept cylinder. The larger maps show strong image-sources located outside the closed test section, generated by acoustic reflections on the walls.

Figure 32 (right side) shows the same maps obtained with the lateral walls covered with liners: the image-sources are now hardly visible outside the test section. On the left side of the figure, we compare spectra measured with the swept cylinder, with/without liners, (i) with one single microphone and (ii) derived from the noise maps after integration in the cylinder area (dotted rectangle). Measurements with the single microphone show that the liners slightly decrease the acoustic levels in the test section, by 5-7 dB. However, it is interesting to see that the integration of the noise maps in the cylinder area is very close

(within less than 1-2 dB) without and with liners, showing that the noise generated by the cylinder is satisfactorily isolated.

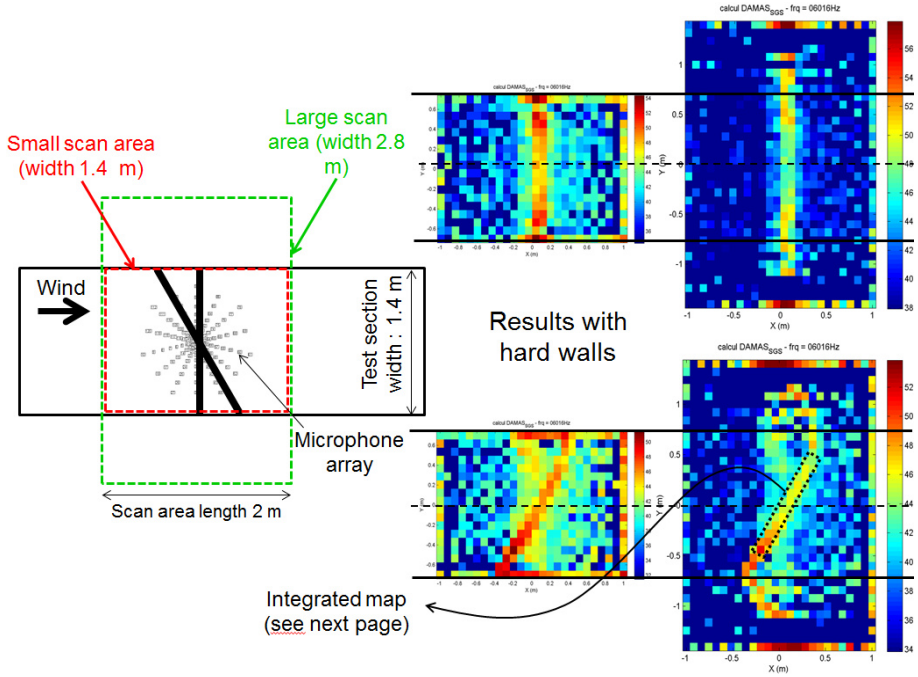

Figure 31 - Left: small and large scan areas. Right: DAMAS noise maps on small (left) and large (right) scan areas, measured with hard walls on straight (top) and swept (bottom) cylinder at 6 kHz

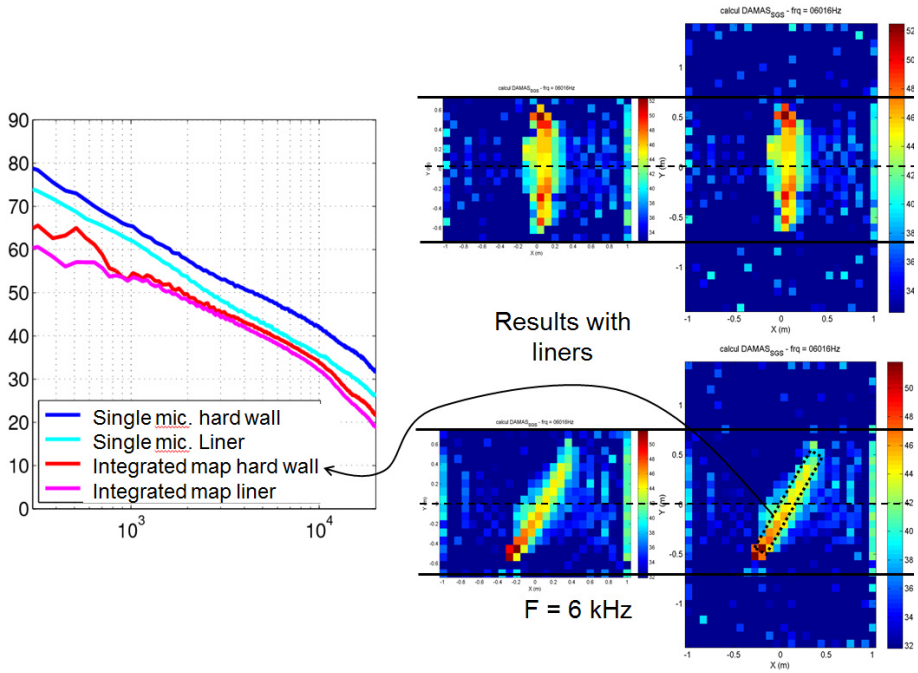

Figure 32 - Right: DAMAS noise maps on small (left) and large (right) scan areas, measured with liners on straight (top) and swept (bottom) cylinder at 6 kHz. Left: comparison of spectra measured with the swept cylinder with/without liners (i) with one single microphone and (ii) derived from the noise maps after integration in the cylinder area (dotted rectangle).

7.5 Acoustic confinement effects for rotating machinery in closed section windtunnel

7.5.1 Propeller

Most examples presented in this lecture are from the "airframe noise" topic, which is certainly influenced

by the author's background. Engine noise experiments are also highly challenging, but with less significant background noise issues, since propulsion simulators (jets, fans, propellers) can be designed in such a way that they dominate background noise. In the other hand, other constraints may require testing these components in closed section windtunnels, for example if flight speed conditions are wanted.
In this context, aeroacoustic tests of a CROR (Counter Rotating Open Rotor) model have been achieved in Onera's S1MA transonic windtunnel located in Modane, France. The propulsor diameter was approximately 0.7 m whereas the WT test section has a diameter of 8 m. The flow Mach number is 0.75. In order to evaluate the acoustic confinement effect for such test, accounting for the convection effects at Mach 0.75, CAA computations have been achieved (*sAbrinA.v0* solver) with the propeller noise source modeled by a circular array of rotating monopoles, pulsating at the propeller BPF (Blade Passing Frequency). Two computations are achieved, one in free field, and another one inside the closed section windtunnel. Figure 33 shows results for a single propeller, in terms of instantaneous and RMS pressure in two planes (axial and transverse). The convection effect induced by the flow at Mach number 0.75 is visible in free field, with an apparent acoustic wavelength 7 times shorter in the upstream direction (0.25 λ_0) than in the downstream direction (1.75 λ_0). Results in the confined configuration are obviously affected by strong reflections on the walls, which generate a complex standing waves pattern. The confinement effect is particularly significant in this case, because the noise radiated by a single propeller is characterized by a single acoustic lobe oriented in the radial direction. For a propeller doublet, an additional component is generated by the aerodynamic interaction between the propellers, with a less directive lobe that should be less affected by the confinement.
Nevertheless, this computation suggests that any attempt to numerically simulate such experimental set-up should mandatorily account for this confinement effect, unless a "de-confinement" method is applied, as it was suggested in the last section.

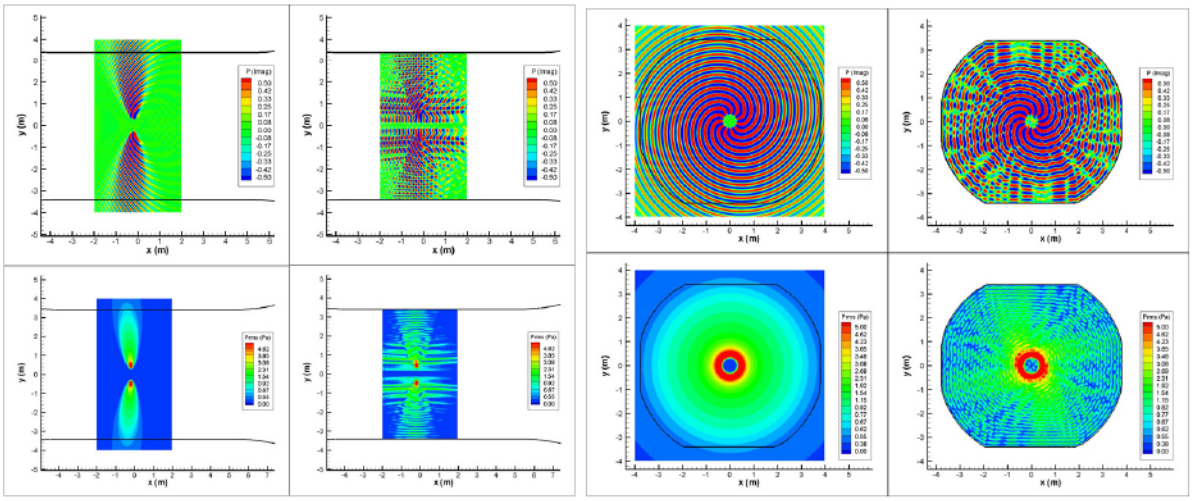

Figure 33 - CAA computations of a propeller model (circular array of rotating monopoles) at Mach number 0.75 in free field and in the S1MA test section. Axial (left) and transverse (right) planes. Instantaneous (top) and RMS pressure

7.5.2 Fan

One objective expressed by European aircraft and engine manufacturers is to build a turbofan aeroacoustic test bench that could be tested in several different windtunnels, including S1MA (see last section) for high speed noise tests. In order to evaluate the influence of the acoustic confinement on the fan noise radiation for such turbofan bench, CAA computations have been achieved with the same methodology as in the last section. This time, the fan noise sources are modeled as a typical acoustic azimuthal mode inside a generic coaxial nacelle. Figure 34 compares results obtained at Mach 0.75 in free field (left) and inside the S1MA closed test section (right). It is interesting to observe that fan noise looks considerably less affected by the confinement effect than propeller noise, as seen on Figure 33.

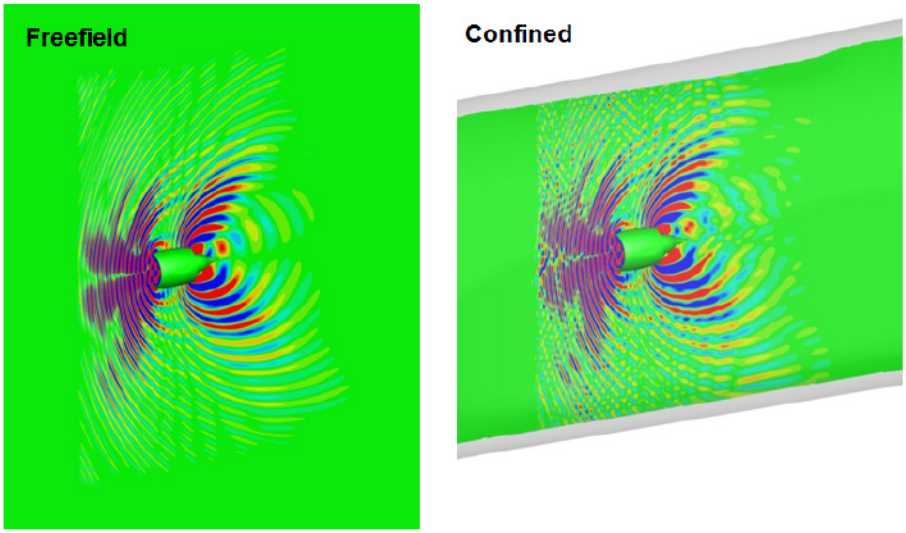

Figure 34 - CAA computations of a fan acoustic azimuthal mode generated in a generic nacelle at Mach number 0.75 in free field (left) and in the S1MA test section (right). Instantaneous pressure in axial plane.

8. EXISTING AIRCRAFT NOISE DATABASES

8.1 Airframe noise

8.1.1 The VALIANT databases

The VALIANT project is based on four test-cases which are of primary interest for the validation of numerical predictions of the noise radiated by airframe noise components such as landing gears and high lift airfoils.

These test cases are (Figure 35):

- turbulent flow over a rectangular gap, tested in AK3 windtunnel at TsAGI ,
- flow past an airfoil with flap, tested in ECL's windtunnel,
- flow past an airfoil with slat, tested in ECL's windtunnel,
- flow past tandem strut, tested in KAT windtunnel at NLR.

The first configuration reflects major features of the multiple local separation zones present on any aircraft, the second and the third are representative of the high-lift wing configuration, and the last flow is representative of simplified landing gear.

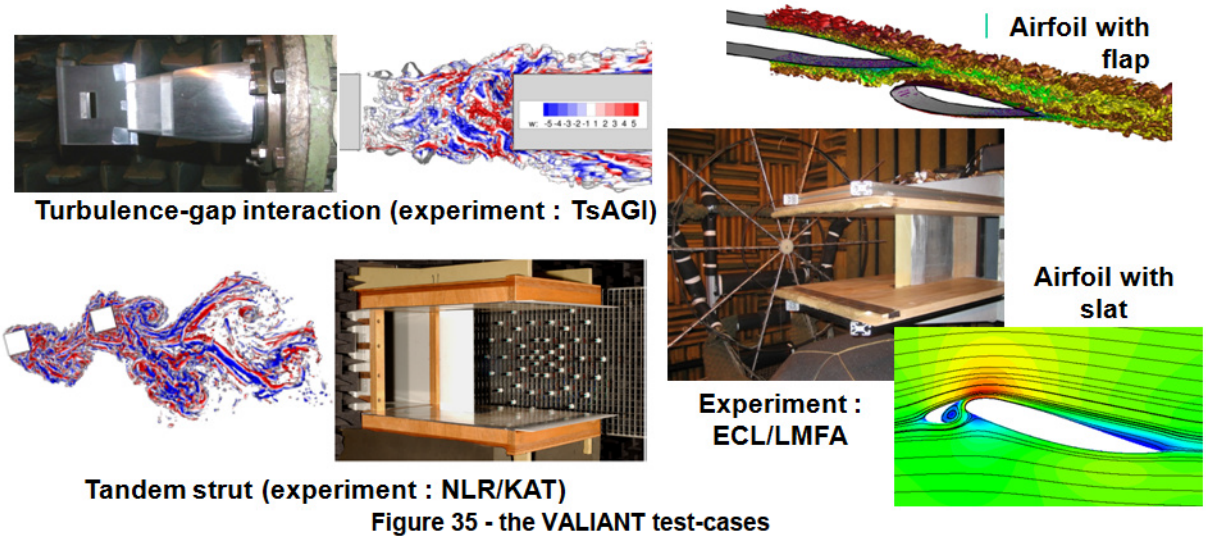

Figure 35 - the VALIANT test-cases

These test-cases were specifically designed under the following constraints:

- they are representative of the most important mechanism of airframe noise generation,
- each test-case tentatively isolates one mechanism from the others,
- all test-cases are specifically adapted to small scale tests in laboratory facilities: the models are simple (and cheap) to manufacture, and designed to (i) minimize the aerodynamic installation effects and (ii) maximize the signal-to-noise ratio.

Each test-case generated an extensive experimental database that has been provided to the partners in the project who planned to achieve corresponding computations. Then one given partner was responsible for collecting the numerical results and provide cross-plotting of these data compared to experimental results and deliver a report.

These databases are not yet available outside the VALIANT project, because it is still under progress and the partners have expressed their concern to wait for the final assessment of the data before to make them public.

Another concern is that the overall benefit of delivery such data would be maximized if it is accompanied by the management and organization of benchmark activities assuming that all contributors (or recipients of the experimental database):

- are clearly identified,
- receive clear requirements in term of numerical results to be generated, and guidelines on how to format these data,
- formally accept to participate to periodical benchmark sessions where results are compared and discussed,

as it is actually done in the BANC benchmark organized by NASA.

8.1.2 The BANC databases

The Benchmark for Airframe Noise Computation (BANC) is an original initiative by the NASA's Aeroacoustics team at Langley Research Center (LaRC). This project has no time limitations and no shared budget (all contributors are self-funded). The idea is to manage a (non exhaustive) list of test-cases for which experimental databases are available and formatted, with written requirements (problem statements) for providing results of numerical simulations. For each test-case, one partner (generally the original owner of the experimental database) is taking care of collecting the results and summarizing the results during benchmark sessions. The first sessions were organized on a yearly periodicity basis, ideally placed just after the annual AIAA/CEAS Aeroacoustics conference: the first session BANC-I was held in Stockholm in 2010, then the BANC-II session in Colorado-Springs in 2011, then the BANC-III session in Atlanta in 2014 and finally, a BANC-IV session in Lyon in 2016.

Up to now, 8 test-cases have been proposed to the community. This list is open, meaning that any new interesting configuration can apply for joining the benchmark, as long as it is complementary with respect to the test-cases already included in the list [15].

The test-cases are currently the following (Figure 36):

1 Simple Airfoils (NACA0012 and DU-96-180) : several tests have been conducted, but at various scales and flow conditions (leader: DLR)
2 In-line tandem cylinder: aerodynamic tests were achieved by NASA in BART, and acoustic tests in QFF (leader. NASA).
3 *Gulfstream Nose landing gear*: aerodynamic tests were achieved by NASA in BART, and acoustic tests in UFAFF (University of Florida) (leader: NASA).
4 Rudimentary 4-wheel landing gear: aerodynamic tests were achieved by Boeing in NAL (India). To our knowledge no acoustic tests have been achieved now (leader: Boeing).
5 LAGOON simplified 2-wheel landing gear: aerodynamic tests were achieved by Onera in F2, and acoustic tests in CEPRA19 (leader: Onera/Airbus) [16].
6 30P30N high lift airfoil (chord 0.46 m): aerodynamic tests were achieved by NASA in BART, but no acoustic tests have been achieved up to now (leader: NASA).
7 LEISA high lift airfoil (chord 0.3 m) aerodynamic tests were achieved by Onera in F2, and acoustic

tests in AWB at DLR (leaders: DLR/Onera) [13].

8 Farfield radiation methods: A) analytical sources: a (provided) Fortran code uses analytic method to provide the acoustic scattering of a quadrupole on a sphere. This code allows to get the acoustic field on any control surface used by integral methods, and then to compare these data with direct solution. B) CFD sources: tandem cylinder flow computed by NASA (CFDL3D solver) is provided (leaders: NASA/Onera/JAXA).

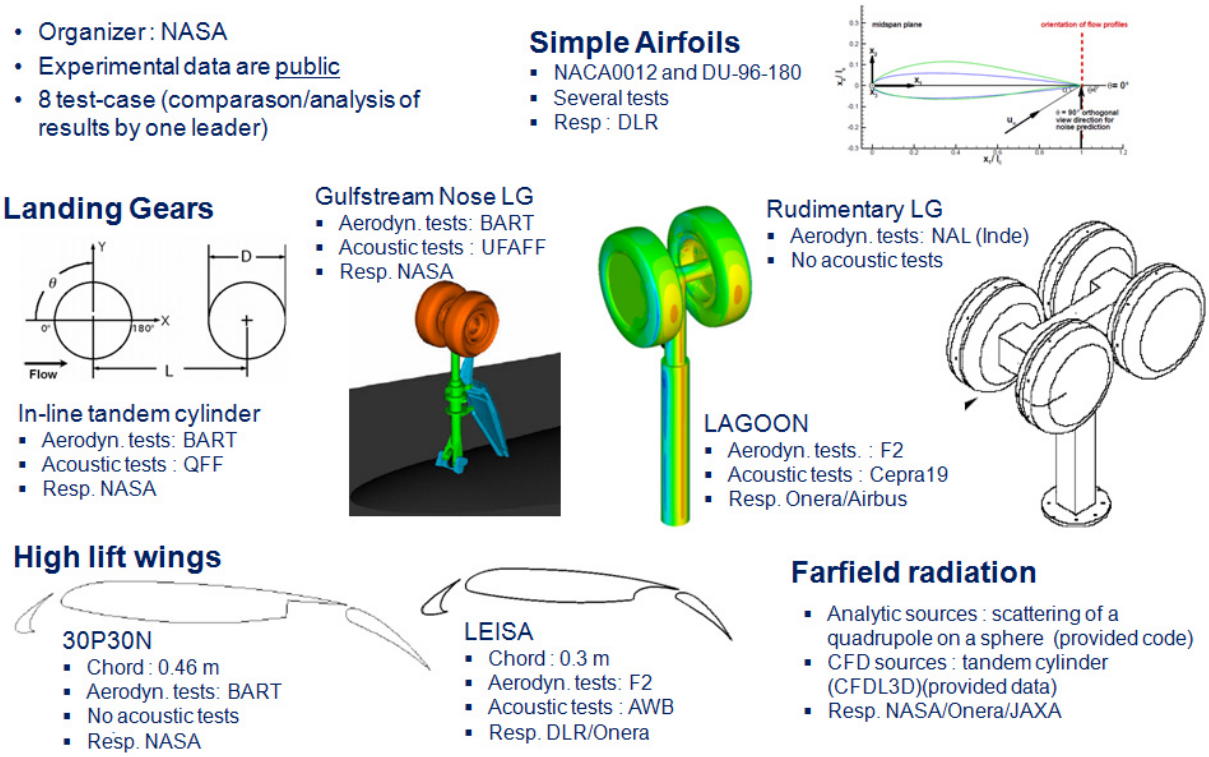

Figure 36 - The BANC (Benchmark for Airframe Noise Computation) test-cases

8.1.3 Cavity : AEROCAV

In the French project AEROCAV, Airbus, ECL and Onera (with several French academic partners) wanted to build an aerodynamic and aeroacoustic experimental database for the evaluation and validation of numerical predictions methods for the unsteady flow and noise of a cylindrical cavity of diameter and depth equal to 0.1 m. Such cavities are commonly found on fuselage and wings of transport aircraft, with specific functionalities which prevent for closing them, so flows past them generate noise and Airbus is willing to understand its physics and then reduce or eliminate this noise source. In AEROCAV, the chosen approach was to test the same cavity in ECL's aeroacoustic windtunnel for acoustic measurements (Figure 5), then in Onera's F2 aerodynamic windtunnel (Figure 3) [6].

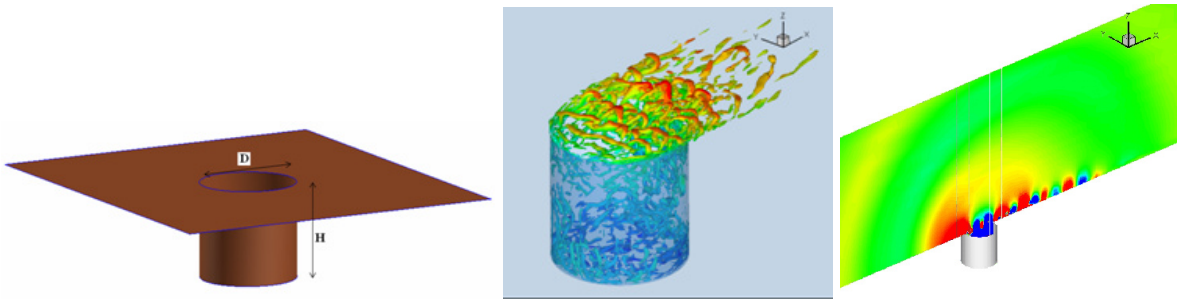

Figure 37 - AEROCAV project : cavity geometry, results of Onera's unsteady flow computation using LES (elsA solver)

These tests have generated an extensive database for several cavity shapes. The AEROCAV project is now completed, and the database is about to be made available by the involved partners (Onera and ECL). The project leader is ECL (C. Bailly). Figure 37 shows the studied geometry and some LES results obtained by Onera (elsA solver) [17].

8.2 Fan noise

8.2.1 Rod/airfoil interaction

Another interesting configuration is the rod/airfoil interaction which was tested at ECL in the framework of the TurboNoiseCFD program, oriented to the thematic of broadband fan noise, a generic configuration which is also representative of physical mechanisms observed in airframe noise [18].

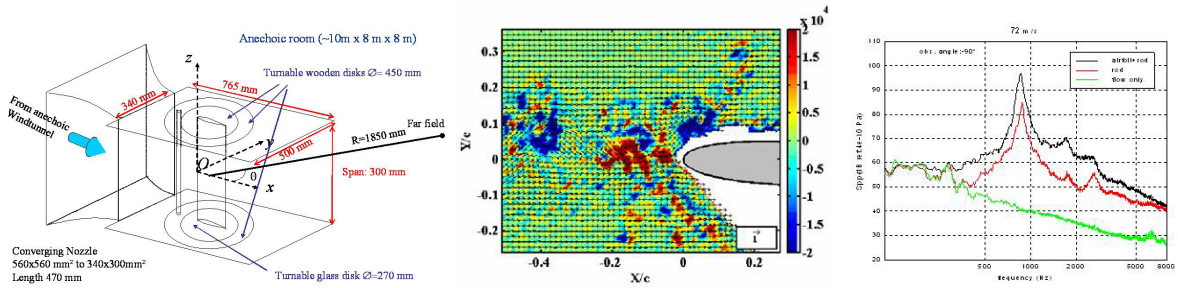

Figure 38 - Rod/airfoil interaction. Test-setup, PIV map and noise spectra (from ECL)

The set-up consists in a cylindrical rod with diameter 10 mm located 105 mm upstream the leading edge of a simple NACA0012 airfoil of chord 100 mm, without any incidence to avoid lift. This 2D configuration is mounted between two end-plates with a total span of 300 mm. The set-up and the available aerodynamic and acoustic measurements (Figure 37) are fully documented by ECL and are available on line [19].

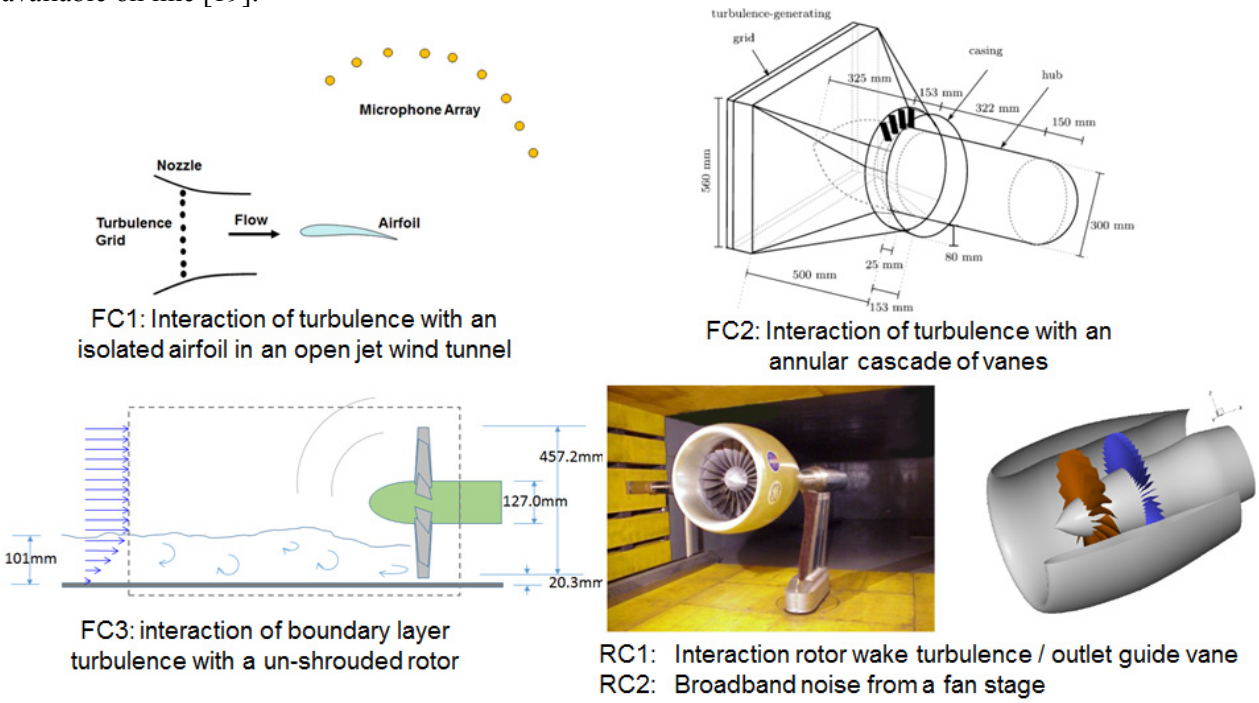

Figure 39 - Fundamental (FC1, FC2 and FC3) and realistic (RC1 and RC2) test cases proposed in the fan broadband noise prediction workshop

8.2.2 Fan broadband noise prediction workshop

Fan broadband noise is a major source of aircraft engine noise, but its accurate prediction remains a challenge. Most existing methods are analytic in nature and rely on simplified descriptions of the flow,

turbulence, and the fan stage geometry to predict sound power level spectra. The high-fidelity numerical simulation tools provide a means for direct prediction of the fan turbulence and resulting broadband noise, but these methods demand substantial computational resources for the complex fan stage geometry and flow.

To identify the shortcomings of existing analytic and simulation approaches, and chart the course of the future research in this important area, the Fan Broadband Noise Prediction Workshop will serve as a forum for assessing the current state of the art, using a portfolio of benchmark problems for which detailed information on the mean flow, turbulence characteristics, and the sound field exist. The current portfolio includes the following fundamental and realistic benchmark cases displayed on Figure 39 :

1. FC1: Interaction of turbulence with an isolated airfoil in an open jet wind tunnel
2. FC2: Interaction of turbulence with an annular cascade of vanes
3. FC3: interaction of boundary layer turbulence with a un-shrouded rotor
4. RC1: Interaction of rotor wake turbulence with an outlet guide vane
5. RC2: Broadband noise from a fan stage

The test-cases description and problem statements are available online [20].

9. CONCLUSIONS

This document is an introduction on the topic of correlating aeroacoustic measurements and numerical predictions of aircraft noise. It is mainly relying on Onera's experience, build over two decades of internal activities and fruitful cooperation with institutional partners in the framework of national and European projects, and through international cooperation projects with laboratories outside Europe.

The need for reliable experimental aerodynamic/aeroacoustic databases has been expressed for a long time. Chronologically, the priority in aircraft noise reduction has been given to engine noise, and especially jet noise research. With the continuous progress in that field, fan noise and airframe noise have more recently become industrial concerns.

This document mainly relies on activities in which the author was directly or indirectly involved, so the presented survey of activities and facilities is far from exhaustive. The main purpose of the lecture is to show that the perfect experiment for validation of aircraft noise prediction does not exist. Any experiment must be adapted to several contradictory constraints, and always results in compromises. The designer of such an experiment has to carefully evaluate all side-effects due to aerodynamic and acoustic interaction effects, or any unexpected interactions between the model, its supports and the facility in which it is tested.

10. REFERENCES

[1] Marcel C. Remillieux, Erin D. Crede, Hugo E. Camargo, Ricardo A. Burdisso, William J. Devenport, Matthew Rasnick, Philip Van Seeters, and Amanda Chou, "*Calibration and Demonstration of the New Virginia Tech Anechoic Wind Tunnel*", AIAA paper-2008-2911, 2008

[2] J. Bulté, R. Davy and Eric Manoha, "*EXAVAC: an experimental programme of unsteady aerodynamics and aeroacoustics for the validation of the numerical simulation of airfoil noise*", AIAA-Paper 2007-3454, 13th AIAA/CEAS Aeroacoustics Conference, 21 - 23 May 2007 Roma (Italy).

[3] Terracol M., Manoha E. and Lemoine B., "*Investigation of the unsteady flow and noise sources generation in a slat cove: hybrid zonal RANS/LES simulation and dedicated experiment*", AIAA Paper 2011-3203, 41st AIAA Fluid Dynamics Conference and Exhibit, Honolulu, Hawaii, 27 - 30 Jun 2011

[4] E. Manoha, J. Bulté, and B. Caruelle, "*Lagoon : An Experimental Database for the Validation of CFD/CAA Methods for Landing Gear Noise Prediction*", AIAA-2008-2816, 14th AIAA/CEAS Aeroacoustics Conference, Vancouver, May 5-7, 2008

[5] E. Manoha, J. Bulté, V. Ciobaca and B. Caruelle", *LAGOON: further analysis of aerodynamic experiments and early aeroacoustics results*", AIAA-2009-3277, 15th AIAA/CEAS Aeroacoustics Conference, Miami, May 11-13 2009

[6] O. Marsden, E. Jondeau, P. Souchotte, and C. Bailly, "*Experimental investigation of flow features and acoustic radiation of a round cavity under subsonic grazing flow*", 7th International ERCOFTAC Symposium on Engineering Turbulence Modelling and Measurements - ETMM7 -4 – 6 June 2008, Amathus Beach Hotel, Limassol, Cyprus.

[7] Nicolas Lupoglazoff and François Vuillot, "*Recent progress in numerical simulations for jet noise computation using LES on fully unstructured meshes*" AIAA Paper 2015-2369, 21st AIAA/CEAS Aeroacoustics Conference 22-26 June 2015, Dallas, TX

[8] D.C. Mincu, E. Manoha, "*Numerical and Experimental Characterization of Fan Noise Installation Effects*" AerospaceLab Journal, Issue 7, June 2014

[9] Amiet R. K.", *Correction of open jet wind tunnel measurements for shear layer refraction*", AIAA paper 75-532, 2nd AIAA Aeroacoustics Conference, Hampton, 1975

[10] Koop, L., K. Ehrenfried, S. Kröber, "*Investigations of the systematic phase mismatch in microphone-array analysis*", AIAA 11th Aeroacoustics Conference, Monterey, USA, May 23-25th, 2005.

[11] C. Kato, A. Iida, Y. Takano, H. Fujita, M. Ikegawa", *Numerical prediction of aerodynamic noise radiated from low mach turbulent wake*", AIAA Paper 93-0145 - 31st Aerospace Sciences Meeting and Exhibit, (1993)

[12] Manoha E., Terracol M., Lemoine B., Le Griffon I., Le Garrec T., "*Slat noise measurement and numerical prediction in the VALIANT programme*", AIAA Paper 2012-2100, 18th AIAA/CEAS Aeroacoustics Conference (33rd AIAA Aeroacoustics Conference) 04 - 06 June 2012, Colorado Springs, CO, 2012

[13] E. Manoha and M. Pott-Polenske, "*LEISA2: an experimental database for the validation of numerical predictions of slat unsteady flow and noise*", AIAA Paper 2015-3137, 21th AIAA/CEAS Aeroacoustics Conference (36st AIAA Aeroacoustics Conference) 22 - 26 June 2015, Dallas, TX, 2015

[14] M. Terracol_ and E. Manoha, "*Wall-resolved Large Eddy Simulation of a high-lift airfoil: detailed flow analysis and noise generation study*", AIAA Paper 2014-3050, 20th AIAA/CEAS Aeroacoustics Conference, 16-20 June 2014, Atlanta, GA, USA

[15] https://info.aiaa.org/tac/ASG/FDTC/DG/BECAN_files_/BANCII.htm

[16] E. Manoha and B. Caruelle, "Summary of the LAGOON Solutions from the Benchmark problems for Airframe Noise Computations-III Workshop", AIAA Paper 2015-2846, 21th AIAA/CEAS Aeroacoustics Conference (36st AIAA Aeroacoustics Conference) 22 - 26 June 2015, Dallas, TX, 2015

[17] D. Mincu, I. Mary, E. Manoha, L. Larchevêque, and S. Redonnet, "*Numerical Simulations of the Sound Generation by Flow over Surface Mounted Cylindrical Cavities Including Wind Tunnel Installation Effects",* AIAA-2009-3314, 15th AIAA/CEAS Aeroacoustics Conference, Miami, May 11-13 2009

[18] Jacob, M., Boudet, J., Casalino, D. And Michard, M. , "*A rod-airfoil experiment as benchmark for broadband noise modeling*.", Theoret. Comput. Fluid Dynamics 19, 171–196, 2005

[19] http://www.lmfa.ec-lyon.fr/perso/Marc.Jacob/Rod_Airfoil_Benchmark.html

[20] http://web1.oai.org/FBNWorkshop.nsf/Index